J Mater Sci

Review

Advances in non-metallic inclusion removal from aluminum melts towards cleaner and higher-performance materials

Bo Yang[1], Semiramis Friedrich[1,*], and Bernd Friedrich[1]

[1] *IME Process Metallurgy and Metal Recycling, RWTH Aachen University, 52056 Aachen, Germany*

Received: 5 May 2025
Accepted: 7 July 2025

ABSTRACT

With the increasing demand for sustainable aluminum materials and the rapid development of high-performance aluminum alloys, the effective removal of non-metallic inclusions (NMIs) from aluminum melts has become a central focus in aluminum metallurgy field and more stringent requirements have been imposed on the content of NMIs in aluminum alloys. NMIs in the aluminum melt will significantly affect the mechanical properties, surface quality and overall performance of aluminum alloys. Aluminum melt purification treatment is the critical step to produce sustainable and high-quality aluminum products. In order to achieve high cleanliness aluminum, various NMIs removal techniques have been developed and continuously improved. This review systematically analyzes the principles and research progress of current NMIs removal techniques, details the influence of different process parameters on the NMIs removal efficiency of different techniques, and highlights the advantages and limitations of each technique. In addition, the key points for future research and development of NMIs removal techniques are also proposed, with a focus on improving purification performance and sustainable development. The aim of this study is to provide a foundational reference for the development of next-generation aluminum purification techniques that enable cleaner, more sustainable, and higher-quality aluminum products for high-performance applications in future high-end industries.

Introduction

According to data from International Aluminum Institute, global primary aluminum production reached 72.9 million metric tons in 2024, with a steady upward trend in recent years [1]. Aluminum and its alloys not only have low density, high yield strength and ultimate tensile strength, excellent fracture toughness, fatigue strength, but also maintain good thermal and electrical conductivity, high corrosion resistance, high ductility and favorable casting properties, etc. [2–7]. These advantageous characteristics have contributed to the widespread and increasing applications of aluminum materials in aerospace, marine vessels, transportation,

Handling Editor: Stephen Eichhorn.

Address correspondence to E-mail: SFriedrich@ime-aachen.de

https://doi.org/10.1007/s10853-025-11195-9
Published online: 20 July 2025

machinery, construction, petrochemicals, food packaging, and other modern industrial fields [8–10].

The rapid development of advanced functional materials and manufacturing industries has led to increasingly complex applications of aluminum, resulting in a growing demand for high-performance Al alloys across various fields and more stringent quality requirements. Enhancing the properties of aluminum materials requires strict control over not only chemical composition and microstructure but also melt cleanliness which is primarily determined by dissolved impurities, dissolved gases (mainly hydrogen) and non-metallic inclusions (NMIs) [11]. NMIs can be classified by their chemical composition as consisting mainly of oxides, carbides, borides, nitrides and salt components [12]. According to the source, NMIs can be categorized into endogenous and exogenous inclusions. Exogenous inclusions come from external sources, such as refractory materials, while endogenous inclusions are formed by high temperature reactions between elements in the melt. Numerous studies have demonstrated that the concentration, morphology, size, hardness, plasticity and distribution of NMIs can directly affect Al processing as well as quality and performance of Al products, including surface integrity, strength, toughness, plastic deformation behavior, corrosion resistance, etc. [13–18]. Due to the high hardness and poor ductility of NMIs, they can easily lead to surface defects such as pinholes, cracks, or even foil fracture during rolling and coating processes, reducing qualification rates, performance, and overall yield of Al foils [19, 20]. The existence of NMIs in the aluminum significantly increases the effective viscosity of the melt and adversely affects the melt fluidity [21, 22]. This can lead to clogging of the casting nozzles and filters on continuous casting lines [23], reduce the efficiency of the feeders, result in porosity in the castings [24–26], and ultimately affect the quality and performance of the castings [27, 28]. Additionally, NMIs have a key effect on porosity formation in aluminum alloy castings, which is ultimately detrimental to their mechanical properties ductility and tensile strength [29]. In John Campbell's Bifilm theory, bifilms, consisting of two oxide layers separated by a thin layer of air or other gases, act as key defect sources, leading to porosity, shrinkage and crack [30–32]. The mismatches between NMIs and the surrounding aluminum matrix material, in terms of stiffness mismatch, strength and ductility mismatch and thermal expansion mismatch [15, 33–35], can induce localized dislocation accumulation and create stress–strain concentration areas adjacent the inclusions [36–38]. These residual stress–strain concentrations are the primary source of microcracks, which impede the plastic deformation of the aluminum alloy, resulting in increased brittleness and dramatically reduced ductility of the material [39, 40].

NMIs have a close interaction with hydrogen, where dissolved hydrogen atoms in the melt tend to adsorb onto the inclusions. Due to its lower solubility of hydrogen in the solid aluminum, NMIs can serve as nucleation sites for precipitation of dissolved hydrogen, which leads to an increase in potential porosity [41–46]. As the contents of NMIs increase, the corrosion potential of Al alloys gradually becomes more negative, leading to a decrease in corrosion resistance of Al alloys [47].

With all this background, the effective removal and control of non-metallic inclusions in the aluminum manufacturing process is a key technology that has been continuously improved and optimized over the last decades. This paper first summarizes the effects of non-metallic inclusions on the properties and performance of Al alloys to highlight the critical importance of optimizing NMI removal processes for an improved final product quality. The current advances in NMI removal processes are then analyzed in detail, discussing the advantages and limitations of each process. The aim of this review is to provide a basic reference for the future development of high-quality aluminum alloys and to promote their application in future high-performance industries.

The development and current status of removal of NMIs in Al melts

A variety of effective techniques have been developed so far for the purpose of removal NMIs, mainly including salt fluxing, sedimentation, gas purging (bubble flotation), electromagnetic separation, filtration and supergravity-enhanced separation. Each individual technique is explained in detail in the following.

Salt fluxing

Salt fluxing process is in general the first cleaning step for aluminum melts and is widely applied in the Al melts purification and Al scrap recycling process. Salt fluxes are generally a mixture of several low melting

point inorganic salts. According to their purpose and function, salt fluxes can be categorized into four main types, including covering fluxes, drossing fluxes, refining fluxes and furnace wall cleaner fluxes [48–50]:

- Covering fluxes form a shielding molten layer on the melt surface, preventing the melt from oxidation and absorption of hydrogen.
- Refining fluxes facilitate the removal of metallic impurities and accelerate the separation of NMIs from the melt.
- Drossing fluxes are applied to promote the separation of aluminum oxide dross from entrapped molten aluminum through exothermic reactions with metallic aluminum, such as $2Al + KNO_3 \rightarrow Al_2O_3 + 1/2N_2 + K$ ($\Delta H^0 = -1230$ kJ). The generated heat enhances flux fluidity, while the liberated potassium reduces interfacial tension and improves wettability, facilitating the coalescence of aluminum droplets. Drossing fluxes effectively reduce the metallic aluminum content in the drosses, which can otherwise reach 60–80% [50].
- Furnace wall cleaner fluxes primarily soften and remove excessive aluminum oxide buildup on the furnace walls, especially near the surface of the melt [51].

The main removal mechanism of suspended NMIs in Al melt via salt fluxing relies on differences in wettability, i.e., NMIs have a higher wettability with molten salts than with aluminum, prompting their spontaneous migration across the Al melt/salt flux interface into the salt flux [52, 53]. As illustrated in the red dashed region of Fig. 1, the suspended NMIs removal process by the wettability of fluxes can be divided into three steps: (I) the suspended inclusions approach to the Al melt/salt flux interface; (II) inclusions migrate to the Al melt/salt flux interface and adhere; (III) inclusions migrate away from the interface towards the interior of the molten salt due to the interfacial tension between the three phases, then float with salt flux to the melt surface, and eventually be absorbed into the molten salt flux layer [54].Additionally, molten salts (e.g., Na_3AlF_6, $Na_2B_4O_7$ and $K_2B_2O_4$) can partially dissolve or disrupt oxides, which destroys their structural integrity, creates discontinuities, and promotes crack propagation. Mechanical stresses generated by the difference in thermal expansion coefficient between aluminum and aluminum oxide and the density difference between α-Al_2O_3 and γ-Al_2O_3, can lead to crack formation in the oxide films. These combined chemical and mechanical effects facilitate the transfer of NMIs from the melt into the salt fluxes [48]. The green dashed region of Fig. 1 illustrates the removal process of the oxide film based on the dissolving or destroying effect: (I) the molten salt is adsorbed on the oxide film; (II) the continuous oxide film is destroyed, partially dissolved, and stripped by the molten salt; (III) the discrete oxide films are wetted and absorbed in to the molten salt fluxes.

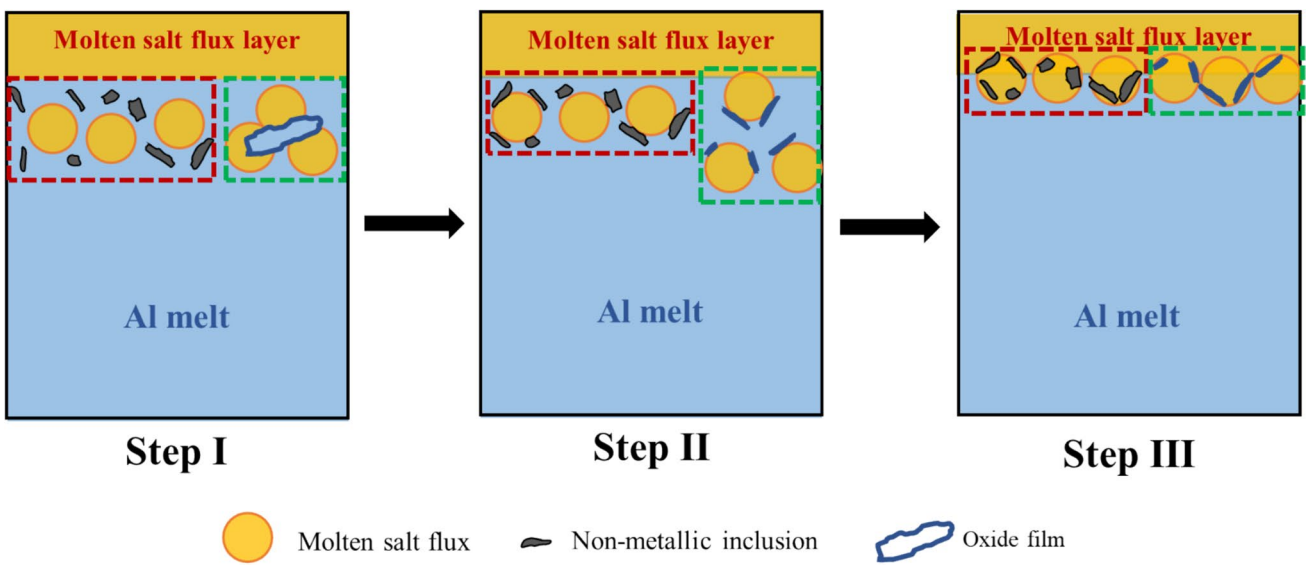

Figure 1 Schematic diagram of the three steps of the removal of non-metallic inclusions by molten [52], modified.

The main factors affecting the performance of this technique are chemical composition, morphology, granularity, quantity of fluxes, refining temperature, time, etc. [42]. In general, salt fluxes can be divided into three main categories based on their chemical compounds, i.e., Chloride-based fluxes, Fluoride-based fluxes and oxidizing compound fluxes.

Chloride salt fluxes are the most basic commercially salt fluxes, typically composed of NaCl and KCl, which can form a low-temperature eutectic at 657 °C [49]. However, due to the limited wetting, adsorption and dissolution ability of chloride fluxes for inclusions, the purification ability and efficiency of chloride fluxes is often enhanced by supplementing fluoride, including monofluorides (e.g., NaF, KF, MgF_2, AlF_3) and double fluorides (e.g., Na_3AlF_6) [49, 54, 55]. The enhancement effects of fluoride are mainly attributed to the following aspects: (1) lowering the melting point of the salt flux mixture with the addition of only a small amounts of certain fluoride, facilitating better fluidity; (2) reducing the interfacial tension between the Al melt and salt fluxes, decreasing the wetting angle between salt fluxes and inclusions and thereby improving the wettability between inclusions and molten salt fluxes [56, 57]; and (3) striping off the oxide layer and dissolving aluminum oxides, thus effectively promoting the separation of NMIs from Al melt and Al coalescence [42, 58–62]. However, fluorides can generate toxic and harmful by-products which cause environmental and ecological concerns. For example, Na_2SiF_6 can partially decompose during salt fluxing process and release SiF_4 gas which can cause serious harm to the surrounding organisms and the environment [63]. Additionally, fluoride salts are also more costly than chlorides, limiting their industrial usage. Consequently, in industrial applications, fluoride additions must be carefully optimized to balance purification efficiency, cost, and environmental impact. In addition to toxic gases contamination, impurities introduced during the salt fluxing process should be carefully monitored. In Al–Mg alloys with high Mg content (> 2 wt.%), sodium-containing fluxes can introduce Na impurities in the form of Na-rich particles in the Al–Mg alloys due to chemical displacement reactions between sodium compounds and Mg, e.g., $2Na^+$ (Salt) + Mg_{Al} (Metal) → Mg^{2+} (Salt) + $2Na_{Al}$ (Metal). Experimental results showed that fluxes containing 0.3 wt. % NaF or Na_3AlF_6 can significantly increase residual Na levels in Al-10% Mg melts, reaching up to 35.1 ppm and 22.7 ppm, respectively [64]. In contrast, 0.3 wt. % NaCl results in a lower Na content (7.9 ppm), indicating that its impact is relatively minor. Furthermore, higher magnesium content in Al–Mg alloys enhances their reactivity with sodium-containing fluxes, increasing the risk of sodium contamination. Excessive sodium content (> 10 ppm) could cause high temperature embrittlement of Al–Mg alloys via intergranular fracture [49, 65, 66]. Therefore, more expensive sodium-free fluxes (e.g., $MgCl_2$-KCl binary flux) are the preferred choice for Al–Mg alloys [51].

Various oxidizing compounds can also be added into the salt fluxes to further enhance the effectiveness of salt fluxing process. Oxidizing compounds, comprising sulfates, carbonates, and nitrates could react exothermically with the aluminum in the dross to raise the temperature of the melt and improve its fluidity and wettability, thereby facilitating the separation of NMIs from melt and promoting chemical reactions between salt fluxes (especially fluorides) and inclusions [49, 59, 67]. Oxidizing compounds such as $Na_2B_4O_7$, $K_2B_2O_4$ facilitate the removal of Al_2O_3 due to their ability to dissolve alumina [49].

Nowadays, salt fluxing technique is commonly utilized in industry for the removal of inclusions and is often combined with Gas purging technique to improve the overall efficiency of NMIs removal. However, it has been reported that the fluxes may occasionally remain in the aluminum castings of products if they are not completely removed during the skimming process, and ultimately reducing the machinability or corrosion of products This happens if they are not completely removed during skimming.[68]. Furthermore, chlorides and fluorides can produce harmful by-products, and the disposal of slag waste presents significant challenges, which contradict the principles of sustainable, green production. This process also has the limitation that only large non-metallic inclusions can be removed, so that small inclusions would remain in the melt. Nevertheless, fine scraps, thin-walled scraps, highly oxidized scraps, bottom ash can only be processed effectively under salt fluxes. Fine or thin-walled aluminum scraps are highly susceptible to rapid oxidation and poor melting behavior due to their large surface area and tendency to capture gases and oxide films. Salt fluxes are essential in these cases to suppress oxidation, enhance thermal conduction, and promote metal droplet coalescence, thereby significantly improving metal recovery [69, 70]. In the industrial treatment of highly contaminated and oxidized aluminum scraps or bottom ash, salt fluxes can protect the molten metal from

further oxidation, chemically dissolve and effectively break up the oxide layer, and promote coalescence of metal droplets, enabling efficient metal liberation and separation [71, 72].

Sedimentation

Sedimentation (also known as settling) is the most traditional and basic purification process in the aluminum industry, which serves as the initial purification step to reduce the load on subsequent refining and filtration steps and lay the foundation for subsequent deep purification. The basic mechanism for removal of NMIs in sedimentation process relies on the density difference between the inclusions and the melt. Suspended NMIs either settle to the bottom or float to the surface of the melt under the influence of gravity or buoyancy, leading to their effective separation from the melt, as illustrated in Fig. 2.

Simplifying the forces model of inclusions in the melt during sedimentation process, i.e., considering only gravity, buoyancy, and drag, the drag force ($F_{D(sphere)}$) and the terminal settling velocity ($v_{P(sphere)}$) of perfect spherical particles with respect to continuous fluid motion in laminar flow (Reynolds number < 2) can be characterized by Stokes' law [74, 75]:

$$F_{D(sphere)} = 3\pi\mu v_P d \tag{1}$$

$$v_{P(sphere)} = \frac{gd^2(\rho_P - \rho_M)}{18\mu} \tag{2}$$

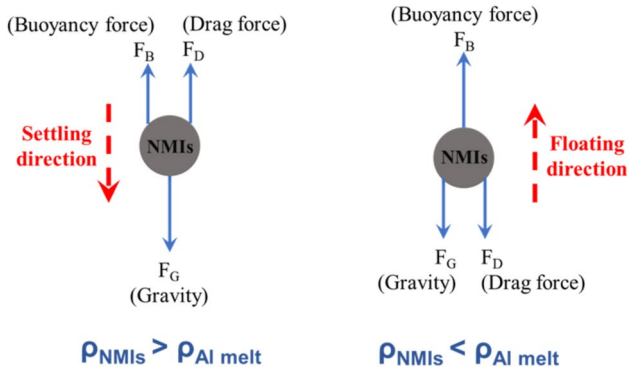

Figure 2 Forces acting on NMIs in Al melt during sedimentation process [73].

where μ is the viscosity of the melt, g is gravity constant, d is the diameter of the spherical inclusion, ρ_P and ρ_M are density of inclusions and melt, respectively.

As illustrated in Fig. 3, the micron-sized inclusions with larger sizes and higher densities have a faster settling speed, which correlates with better removal efficiency [73, 75–77]. Kolsgaard et al. [78] and Ordjini et al. [79] studied the settling behavior of SiC inclusions in Al melt. It was found that the settling rate of SiC increased with decreasing particle volume fraction, increasing particle size, and increasing melt temperature. Heidary et al. [80] developed a computer program to predict the settling behavior of SiC in Al/SiC slurries by MATLAB software, which incorporated simple Stokes' law with some relevant correction factors to consider the effect of slurries viscosity and particle shape, thereby improving the accuracy of the NMIs settling velocity prediction. TiB_2 is an important nucleation substrate for grain refinement in aluminum alloys, but it is also a major non-metallic inclusion belonging to the borides group. Due to its high density (4.52 g/cm^3), TiB_2 is highly suitable to be removed by sedimentation process, and its settling behavior in Al melts has been widely studied in various literature [81–83].

In practice, non-metallic inclusions in aluminum melts are typically non-spherical particles, mostly in polygonal or irregular shapes. The shape factor affects the drag force acting on the particles thus having a significant effect on the NMIs settling behavior,

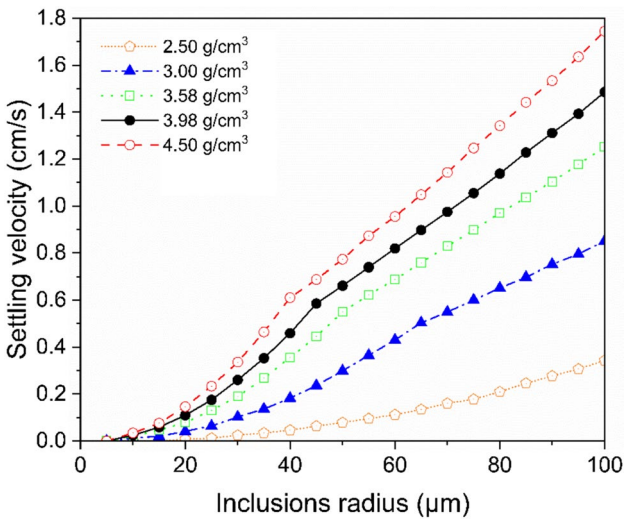

Figure 3 Settling speed as a function of radius and densities of inclusions in the Al melt [75], modified.

which can be described by the drag coefficient (C_D) of the particles [73, 84, 85]. Gökelma studied the settling behavior of spherical-like and thin-film Al_2O_3 inclusions in Al melts, and concluded that the diameter is positively correlated with the settling velocity, whereas the aspect ratio of NMIs is negatively correlated with the settling velocity [76]. By geometrically approximating the inclusion film by a non-spherical thin disc with a certain aspect ratio, the terminal settling velocity of the film in the Al melt can be calculated as [76, 77]:

$$v_{film} = \frac{(\rho_P - \rho_M)\pi dhg}{32\mu} \tag{3}$$

where ρ_P and ρ_M are density of inclusions and melt, d is the diameter of the film inclusion, h is the thickness of the film inclusion, g is gravity constant, μ is the viscosity of the melt.

In a real situation of the melting process of aluminum, natural- as well as forced convection inevitably occur and cause a dual effect on the removal of inclusions. The poor wettability between non-wettable NMIs and Al melt promotes collisions and aggregation of NMIs, which should be considered in the study of the kinetic behavior of NMIs in the melts [86]. Convection such as turbulence flow benefits the agglomeration of non-metallic inclusions into large-sized clusters by actively colliding with each other, thus enhancing their settling or floating behavior [87–89]. The simulation results showed that the inclusions clusters were formed very fast under turbulence and their formation kinetics followed a second-order behavior in the early stages of agglomeration [90]. Brownian (random motion), Stokes (creeping motion) and turbulent collisions all affect the agglomeration of non-metallic inclusions. Turbulent and Brownian collisions become more active with increasing melt convection, while Stokes collisions have the opposite effect [91]. Agglomeration contributes to the formation of larger clusters of non-metallic inclusions, which plays a vital role in improving the separation efficiency of non-metallic inclusions in sedimentation and bubble flotation processes. However, natural convection and forced convection disturb the melt which have negative effects on the settling behavior of suspended inclusions. Irons et al. [92] monitored the in-situ settling behavior of 14 μm SiC particles in an Al-Si melt by an electrical resistance probe, and the results showed that significant agglomeration occurred before settling begins and that mechanical stirring would break up the agglomerates and reduce the settling velocity of clusters. The geometry of the furnace has a significant effect on fluid flow and particle settling behavior [93]. Sztur et al. [74] developed a numerical model to calculate turbulence fluid flow, inclusion trajectories, and settling velocities of inclusions in a laboratory-scale furnace and an industrial-scale furnace. Theoretical calculations showed that the maximum flow velocity of natural convection in a 35t industrial furnace is with 13 mm/s significantly greater than the 3 mm/s in a 1t lab-scale experimental furnace. Both model calculations and experimental data indicated that large inclusions (100 μm in diameter) were not significantly affected by natural convection. However, small inclusions (10–40 μm in diameter) can be trapped in the vortex (or natural convection), thus making it difficult to settle. The extent to which inclusions are affected by natural convection depends on the comparison between the diameter of inclusions (d) and Stokes diameter (d_{Stokes}) [73, 77]. d_{Stokes} refers to the inclusion diameter where the Stokes velocity of inclusion is identical to the velocity of the melt. For large particles ($d > d_{stokes}$), the sedimentation behavior of NMIs is quite in accordance with Stokes' law (see Eq. (2)) and is not greatly affected by natural convection. For small particles ($d < d_{stokes}$), however, NMIs are entrained by natural convection at near-fluid velocities. In addition, NMIs suspended in Al melt can undergo random thermal collisions with liquid molecules, which creates unbalanced Brownian force on the particles, leading to irregular Brownian motion of the particles in a zig-zagged trajectory [94]. According to the Stokes–Einstein equation, the Brownian diffusion coefficient of particles is inversely proportional to the size of the particles, meaning that as the particle size increases, the Brownian motion of particle becomes slower and less noticeable. For larger inclusions (diameter > 10 μm), the Brownian motion has a negligible impact on their trajectories [90].

To summarize, the sedimentation process has the advantages of simple process, no need for complex equipment, low operating costs and suitability for large-scale industrial applications, making it suitable for the initial purification of Al melts. Based on the density data of the aluminum melt and non-metallic inclusions [95], it can be theoretically predicted that NMIs with density greater than the aluminum melt can be effectively removed by the settling mechanism. Nevertheless, certain NMIs (e.g., Al_4C_3 with a density

of 2360 kg/m^3) that approximate the density of melt are challenging to remove by sedimentation. Precise control of melt temperature is critical, as excessively high melt temperature promotes the formation of oxides, while excessively low temperatures increase melt viscosity thereby hindering the settling of inclusions. In addition, when the size of inclusions is extremely small (d < 10 μm), the settling velocity of inclusion becomes negligible or even inhibited due to the influence of convection or Brownian motion, resulting in a low NMIs removal efficiency. Consequently, the sedimentation process is generally applied in industry to remove inclusions with large diameters and high differences in density from the melt. In addition, since the sedimentation process becomes significantly prolonged for fine particles or those with densities close to that of the melt, the settling process in the industrial field for non-metallic inclusion removal in aluminum melts requires careful optimization of treatment time to balance NMIs removal efficiency and economic feasibility.

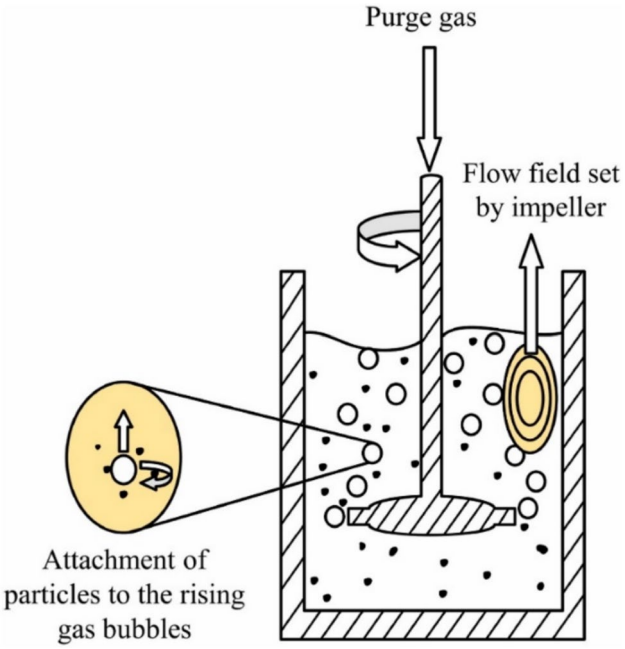

Figure 4 Schematic diagram of the gas purging process to remove inclusions [102].

Gas purging (bubble flotation)

Gas purging technique, which can also be termed as bubble flotation, is an effective method for reducing the content of gases (mainly H_2), alkaline elements (e.g., Na, Li), alkaline earth metals (e.g., Ca) and inclusions in the Al melt [96]. During bubble flotation process for melt purification, inert gases (e.g., Ar, N_2, etc.), insoluble active gases (e.g., Cl_2, C_2Cl_6, C_2Cl_4, etc.) or mixtures of both are injected into the melt [11]. Stirring, gas introduction technology and the mass flow of gas are typically optimized to promote melt convection and diffusion in order to produce finer, more dispersed and more uniformly distributed gas bubbles, thereby increasing the gas–liquid interface ratios and ultimately improving the purification efficiency of the process [97]. While the fine bubbles continue to expand and float upward, the bubble surface adsorbs or captures the inclusions from the melt with the interaction between bubbles and inclusions. This process transports the inclusions to the melt surface where they accumulate and are subsequently removed from the melt. The schematic diagram of the gas purging process for removal of inclusions via a rotor is shown in Fig. 4. In a broad sense, the mechanisms of NMIs removal by gas purging technique can be categorized into three main modes: (a) inclusions attached to the bubble surface; (b) inclusions are captured by the rising wake of the bubble; (c) inclusions are dragged by the bubble plume caused by the flow pattern [98–100]. Among them, the bubble surface adsorption mechanism plays a more dominant role [101].

Zhang and Taniguchi [103] proposed a kinetic mechanism of the adsorption interaction between bubble and inclusion, which laid the theoretical foundation for the removal of non-metallic inclusions from melts by bubble flotation process. The overall process of bubble-attached inclusions flotation mainly consists of six subprocesses, as shown in Fig. 5a [104].

As illustrated on the kinetic mechanism perspective, the attachment and capture of inclusions by bubbles and their stability determine the feasibility and efficiency of the bubble flotation process for inclusion removal. Falsetti et al. [104] further revealed the adsorption effect of bubbles on inclusions from a thermodynamic perspective. The relationship among the particle energies (adsorption energy ΔE_a, desorption energy ΔE_d, and attachment energy ΔE_{att}), the contact angle (θ), and the attachment stability of solid spherical particles at the gas–liquid interface was investigated [104–107]. The contact angle (θ) formed between the liquid–gas and solid–liquid interfaces characterizes the wettability of the particle and describes the position of the solid particle. The inclusion has different energy states from the liquid melt to the adsorption

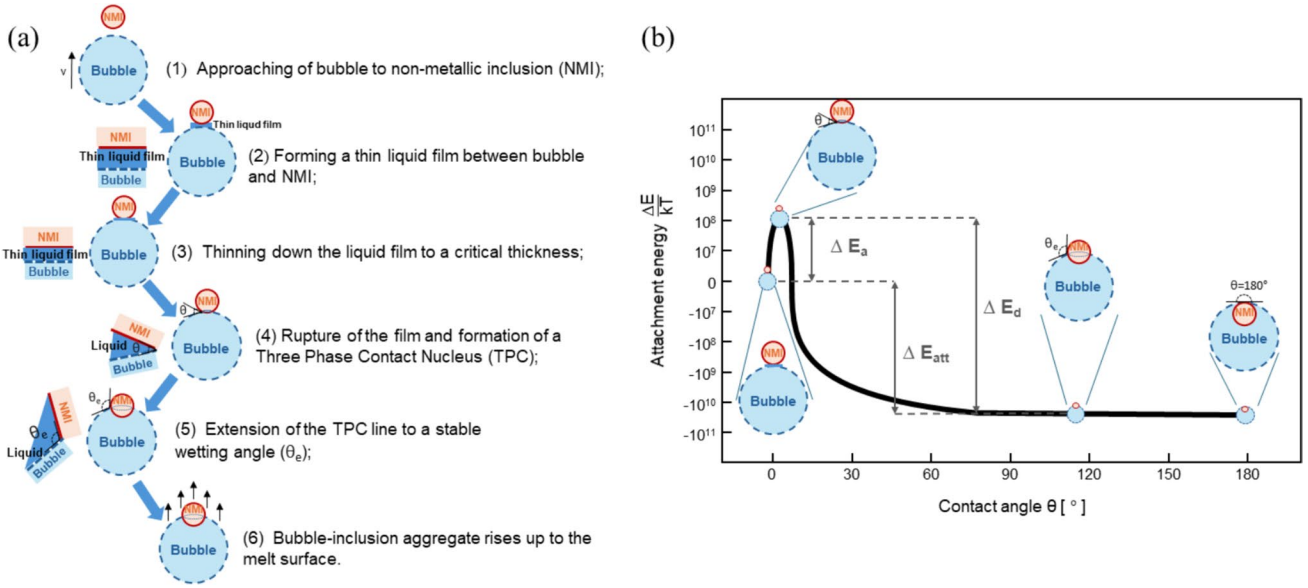

Figure 5 (**a**) Subprocesses of inclusions removal by gas purging process (**b**) Energy of particle attachment to bubble as a function of contact angle [103, 104], modified.

at different positions onto the gas bubble of the liquid–gas interface, as shown in Fig. 5b.

In addition to the terms discussed above, gas purging is an integrated engineering process that is influenced by several factors, including operational-, chemical-, and hydrodynamic factors [108]. Operational parameters such as immersion depths of impeller, impeller rotational speed, impeller geometry, purging gas flow rate, treatment time, melt temperature, bubble size, bubble dispersity and inclusions size all influence the removal of inclusions [109–113]. From a hydrodynamics point of view, the NMIs removal process by gas purging process is a complex flow system of multiple phases interactions, including liquid-phase melt turbulence generated by gas flow and impeller rotation, interactions between liquid melts and purged gas phases, collision dynamics between solid particles, and etc. Impeller rotation speed and gas purge flow are the most important factors on flotation efficiency. Both can create turbulence inside the melt, alter the size, dispersion and volume fraction of the bubbles in the melt, thus affecting the interactions between the multiphase fields and controlling the transport and collision of particles to the bubble surface [102, 114–117]. Mathematical models have been developed to simulate the turbulent multiphase (gas–liquid-solid phase) flow field in the rotating flotation process and the removal of inclusions [114–116]. The simulation results show that the increase in gas purge flow and impeller rotation speed contributed to the effectiveness and efficiency of particle removal. Among them, the impeller rotation speed has the most prominent effect on the performance of gas purging for inclusions removal. On the one hand, the turbulence generated by the high-speed rotating impeller significantly increases possibility of collisions among inclusions, promoting the aggregation of randomly distributed inclusions into relatively larger clusters, which enhances their tendency to either float or settle. On the other hand, the high-intensity of turbulence also facilitates the attachment of particles to gas bubbles, thereby promoting their upward flotation. A higher purge gas flow rate combined with a faster impeller rotation speed enhances the volume fraction of gas in the melt and promotes the purge bubbles to split into bubbles with a smaller average stabilized bubble radius. The smaller the bubble radius, the bigger reaction surface, hence higher efficiency of the removal of inclusions. Therefore, micro-bubble flotation enhances the removal of fine non-metallic inclusions by generating microbubbles (less than a few hundred microns in diameter), which provide greater total surface area per unit gas flow rate high surface energy, and longer residence time, thereby improving attachment and flotation efficiency of NMIs [118–121]. This results in greater collision rates between NMIs and bubbles

and more efficient inclusions removal efficiency [102]. However, at high impeller speeds, the gas flow rate had no significant effect on the inclusion removal efficiency. The geometrical design and depth position of the impeller are important process parameters to optimize the aluminum purification process, which can affect the size and dispersion of the bubbles in the melt, thus affecting the NMIs removal efficiency [122–125].

The inclusions flotation kinetics are highly dependent on size of inclusions [102, 126]. Gas purging process can remove larger particles more efficiently. The smaller size of the inclusions means that they are more difficult to remove. When the size of inclusions is less than 5 μm, the removal degree was basically close to 0%. In industrial applications, gas purging technology can effectively remove inclusions approximately larger than 20 μm in diameter. The addition of chlorine-containing gases improves the removal of NMIs such as TiB_2, Al_4C_3, and oxide films, especially for oxide films suspended in the melt due to fact that the reactive gases can affect the surface tension of the bubbles [127]. Gökelma et al. [128] introduced the Ar-H_2O gas mixture into aluminum melts, and the results showed that the formation of Al_2O_3 or oxycarbide on the surface of H_2O-containing bubbles promoted the attachment of Al_4C_3 inclusions to the bubbles, thus improving the removal efficiency of NMIs.

The gas purging method is simple and effective for the industrial continuous removal of hydrogen and non-metallic inclusions from Al melts. Gas purging method is often combined with salt flux treatment, which can greatly improve the inclusions removal efficiency [129–131]. However, this method has limited ability to remove ultrafine (submicron) NMIs. In addition, the quality of the melt may be negatively affected when the parameters of the gas purging process are inappropriate. For example, when the impeller speed is too fast, the local surface vortex around the impeller and the splashing around the vessel wall can entrain the oxide film from the melt/air interface into the melt [43, 110, 132]. Inert gases (e.g. high purity Ar) are relatively costly to use. In contrast, N_2 gas is more economical. However, gas purging with N_2 can lead to the formation of numerous small-sized nitride bifilms [129, 133, 134]. The increase in NMIs content during nitrogen purging can be attributed, on the one hand, to the chemical reactions between N_2 and alloying elements such as Al and Mg at high temperature, leading to the formation of nitride bifilms such as AlN and Mg_3N_2 [12]. On the other hand, the potential contaminations in the purging gas, such as O_2 and H_2O can also lead to a degradation of melt quality by introducing additional inclusions [129].

Electromagnetic separation

Electromagnetic (EM) separation, an emerging physical separation method, has been extensively studied for removing inclusions [135]. The fundamental mechanism of the electromagnetic separation of inclusions in the melt is mainly to utilize the difference in electrical conductivity between the melt and suspended non-metallic inclusions [136]. When an electromagnetic field is applied to the melt, the molten metal with strong electrical conductivity is affected by the Lorentz force to move in a certain direction. The compression of the molten metal by the Lorentz force generates a pressure gradient within the metal. Most NMIs are electrically non-conductive ($\sigma_p = 0$) or have much lower electric conductivity compared to the molten metal ($\sigma_p/\sigma_f \ll 1$), where σ_p and σ_f represent the electrical conductivities of the inclusions and the molten metal, respectively. NMIs experience a net electromagnetic separating force, often referred to as electromagnetic repulsion or electromagnetic pressure force, which acts in the opposite direction of the Lorentz force acting on the molten metal, thereby promoting their separation from the Al melt, as illustrated in Fig. 6 [135, 137, 138].

The phenomenon of electromagnetic fluid flow in electric and magnetic fields, as well as the forces acting on the spherical and cylindrical inclusions suspended in a conducting fluid and the kinetic behavior of particles was first studied by Kolin in 1953 [139], and subsequently by Leenov and Kolin in 1954 [140]. They proposed the principle of electromagnetic action for separating the non-conductive particles from an electrically conductive fluid, as well as the theoretical equations for the forces acting on the particles. This provided the theoretical basis for the purification of molten metals by electromagnetic separation. The Lorentz force on the melt can be expressed by:

$$F_l = J \times B \tag{4}$$

where F_l (N/m^3) is the electromagnetic force per unit volume of melt, B (T) is the magnetic flux density vector, and J (A/m^2) is the induced current density.

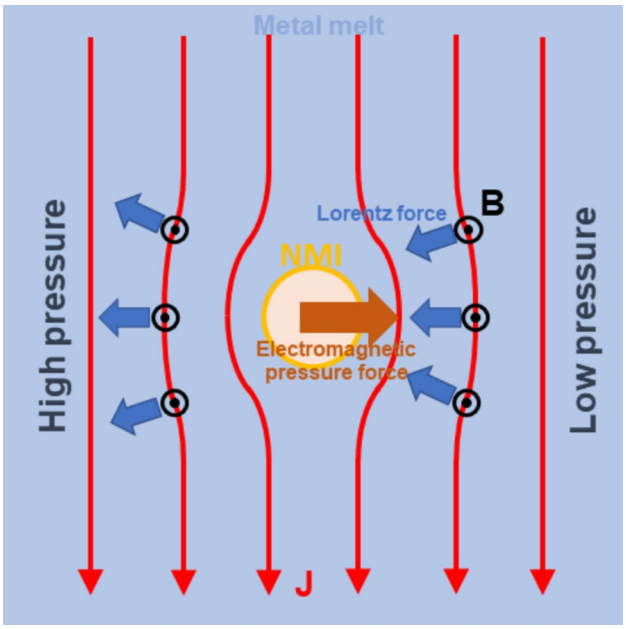

Figure 6 Schematic diagram of the electromagnetic force on non-metallic inclusions and the Lorentz force on the melt [138], modified.

Under the magnetic field and electric field, the electromagnetic force per unit volume on NMIs with different sphericity at low flow velocity in an electrically conducting fluid is [140, 141]:

$$F_i = -\frac{3}{2}\xi\frac{\sigma_l - \sigma_i}{2\sigma_l + \sigma_i}\frac{\pi d_i^3}{6}F_l \tag{5}$$

where F_i (N/m^3) is the electromagnetic force per unit volume on NMIs, ξ is shape factor of non-spherical particles, σ_l (S/m) and σ_i (S/m) is respectively electrical conductivity of liquid melt and inclusions, d_i (m) is the diameter of the particles, and F_l (N/m^3) is the electromagnetic force per unit volume of the liquid melt.

It is evident that high-frequency alternating current (AC) passing through the induction coil generates an alternating magnetic field. The induced currents in the metallic liquid generate an electromagnetic force on the melt under the aforementioned magnetic field. This force is consistently directed towards the center of the liquid metal. Inversely, the inclusions in the liquid metal suffer from a force that is opposite to the electromagnetic force of the melt (see Fig. 7) [142]. This effectively results in the separation of the inclusions in the aluminum melt.

In a high-frequency alternating magnetic field, the balancing interaction between the electromagnetic separation force and the dispersion force due to turbulent flow can migrate and accumulate the particles towards the side walls of the crucible in a very short time (seconds to tens of seconds), leading to the formation of a few-mm-thick layer of particles on the walls [138, 143, 144].

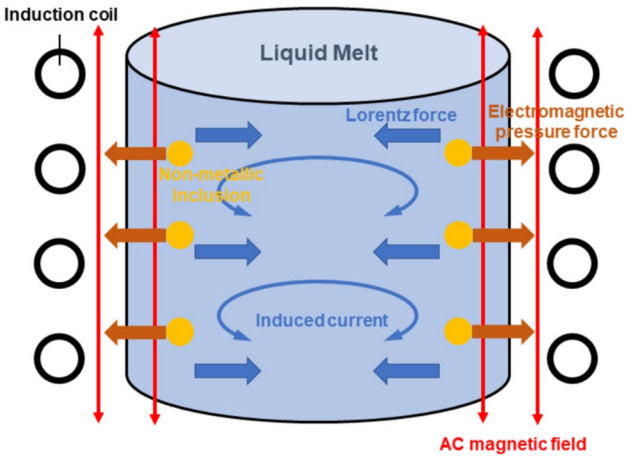

Figure 7 Schematic diagram of an induction coil (alternating magnetic field) for the separation of non-metallic inclusions [142], modified.

The thickness of the inclusion accumulation layer depends on various factors, mainly limited by the depth of the electromagnetic skin. The electromagnetic skin depth refers to the depth within the conductive melt where the induced current and associated electromagnetic force are significantly concentrated due to the skin effect. As the coil current increases, the layer gets thinner and more non-metallic inclusions accumulate at the layer. The lower the crucible wall temperature, the more the liquid metal gets more viscous close to the crucible wall, which helps the inclusions to stick to the crucible wall and overcome the skin depth effect [143]. The removal efficiency (η) of inclusions in Al melt during alternating electromagnetic field is most efficient while the ratio of pipe radius to skin depth (r/δ) ranged from 1.5 to 3, as shown in Fig. 8 [144, 145]. The induced secondary flow of the melt can accelerate the NMIs removal efficiency [146]. With suitable process parameters of alternating electromagnetic field, the removal efficiency of NMIs with a diameter of larger than 5 μm can exceed 90% [147].

A series of studies have been conducted aiming to improve the removal efficiency of NMIs by adjusting the electric and magnetic fields. Depending on

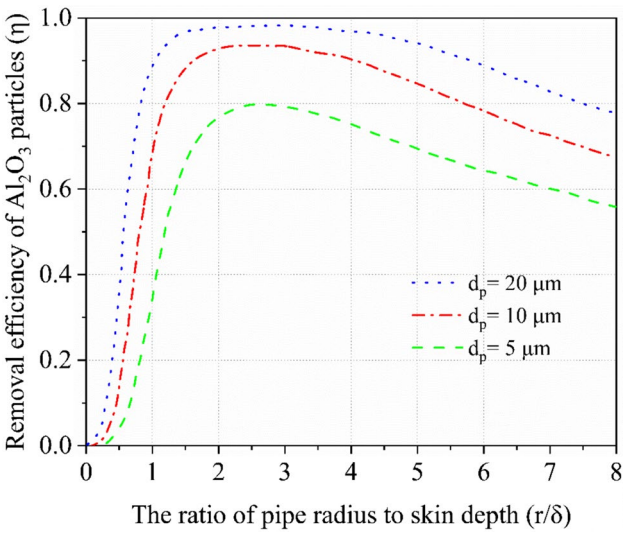

Figure 8 Effect of the ratio of pipe radius to skin depth (r/δ) on theoretical removal efficiency (η) for different particles diameter (d_p) (t = 10 s, r = 5 mm, B = 0.12 T) [144], modified.

the different source of electromagnetic force, electromagnetic fields that have been proposed for electromagnetic separation technique to remove NMIs in aluminum melt can be divided into several categories: stationary magnetic field [148], alternating magnetic field [145, 146, 149–153], rotating magnetic field [154], traveling magnetic field [155–157], high gradient magnetic field [148], superimposed magnetic field such as stationary magnetic field simultaneously imposed with direct current field [145, 158, 159], alternating magnetic field simultaneously imposed with alternating current field [160], and etc. The forces and accumulation position of non-metallic inclusions in liquid metal under different electromagnetic fields are shown in Fig. 9.

Compared with other conventional melt cleaning techniques, the advantages of EM separation technology are (1) strong purification efficiency and performance even for micron-sized inclusions, this

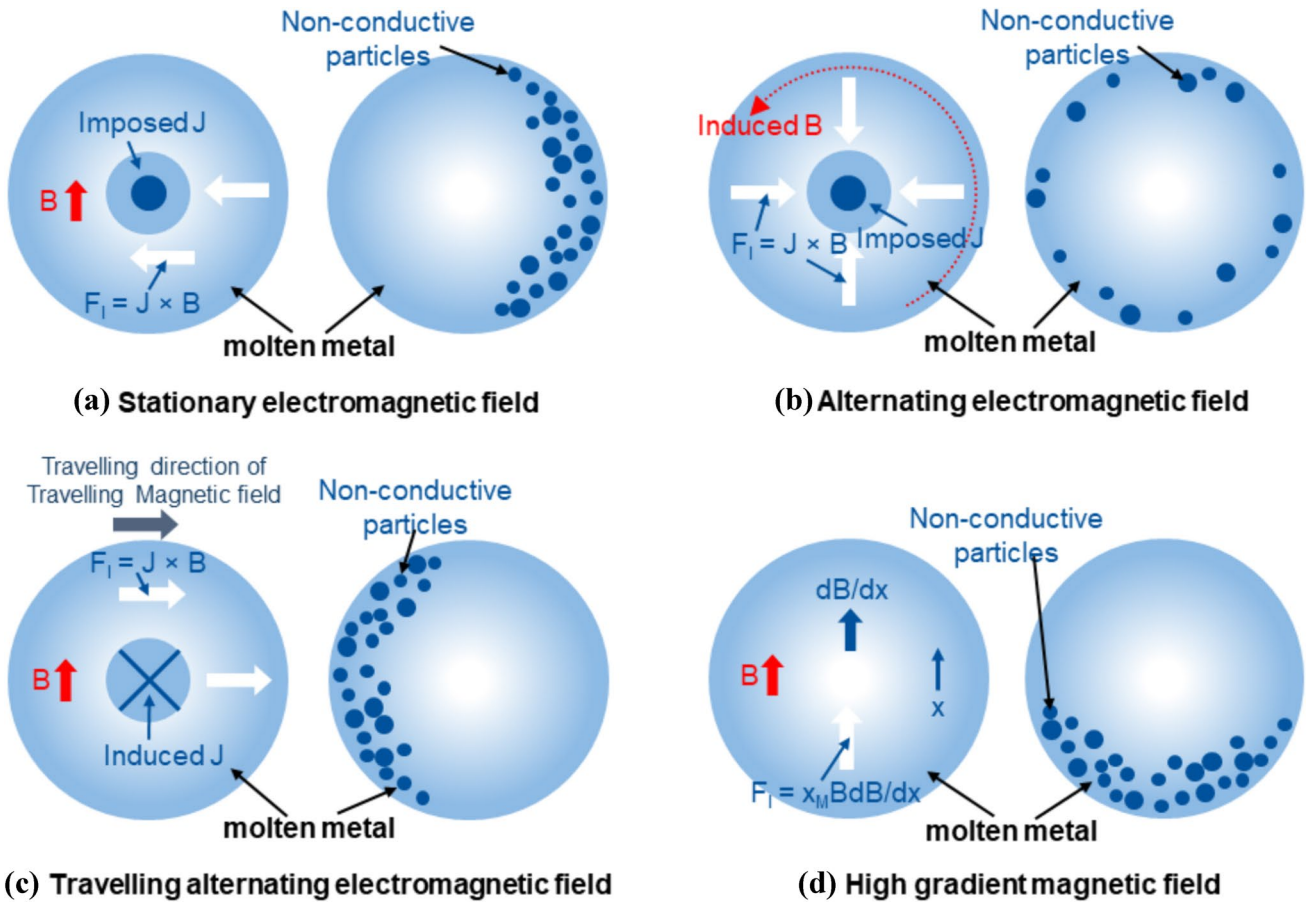

Figure 9 The force and accumulation position of non-metallic inclusions in liquid metal under different electromagnetic fields: **a** stationary electromagnetic field; **b** alternating electromagnetic field; **c** traveling alternating electromagnetic field; and **d** high gradient magnetic field [161], modified.

technique can completely remove inclusions larger than 10 μm, and remove more than 90% of inclusions larger than 5 μm in a short time (a few tens of seconds) [147]; (2) no exogenous contamination, due to the inherent non-contact characteristics of the electromagnetic field, there is no direct contact between the melt and the magnetic field generator, thus avoiding contamination by extraneous contaminants; (3) environmentally friendly, EM separation avoids the use of fluxes compared to salt fluxing technique and avoids the use of argon or chlorine gas compared to gas purging technique. There is no requirement to deal with waste materials and exhaust gases that could cause environmental pollution. However, EM separation technique also has some disadvantages such as (1) limitation in the application scenarios due to the skin effect, especially in alternating magnetic field, which makes it difficult to achieve a large and homogeneous electromagnetic force density within a large volume melt; (2) electromagnetic forces can inevitably lead to convection flow of the molten metal, which adversely affects the separation of inclusions, especially small inclusions, and limits the further development of this technique [137]; (3) from an economic point of view, the cost of EM separation would be higher than that of other purification technologies (e.g., general filtration, bubble flotation, and sedimentation) [135].

Filtration

Filtration is a state of the art, usually used as the final step for removing NMIs prior to casting. During the filtration process, the aluminum melt passes through a filter made of neutral or reactive material. The second-phase particles including inclusions in the melt can be physically or chemically adsorbed by the filter and retained in the filter medium and being separated. There are various types of commercially filters, including ceramic foam filters, deep bed filters, rigid media filters, bonded particle filter, two-stage filter systems, surface-active filter systems, etc. [162, 163]. Among them, ceramic foam filters (CFF) have been widely utilized in inclusion removal process due to their manufacturing simplicity, low cost and high filtration performance [164].

In general, the main mechanisms for removing inclusions by molten metal filtration can be categorized into three different modes, i.e. sieving, cake-mode filtration and deep-bed filtration [165] as shown in Fig. 10. These three filtration modes can work simultaneously or individually to achieve the highest efficiency of solid particles removal. When the aluminum melt contains large-sized inclusions that are comparable to or larger than the size of filter pores, the filtration mechanism primarily operates in the sieving mode, resulting in the inclusions being retained on the filter inlet. As the filtration process continues, inclusions intercepted by the filter surface

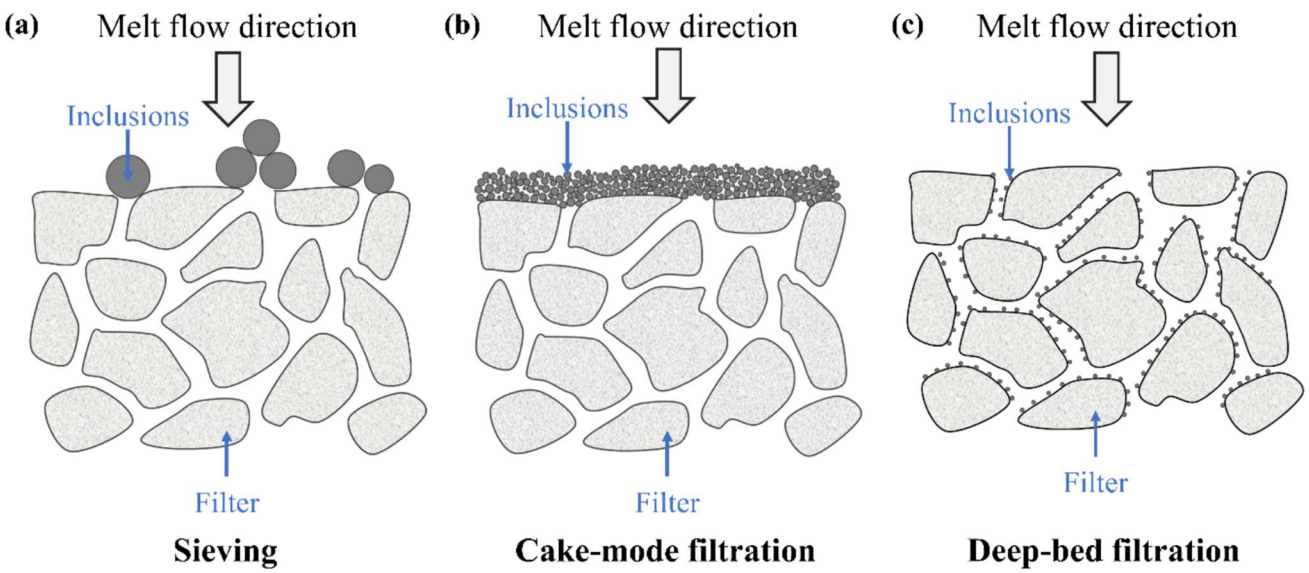

Figure 10 Scheme of the three filtration modes: **a** sieving, **b** cake-mode filtration, **c** deep-bed filtration [165], modified.

gradually accumulate on the filter inlet to form a cake layer [166]. In this scenario, as shown in Fig. 10b, the filtration mechanism begins cake-mode filtration. The subsequent inclusions in the Al melt, both larger or smaller than the diameter of filter pores, can be effectively captured by the previously formed cake layer. The filtration performance in cake-mode filtration progressively enhances as the thickness of the filter cake layer increases. However, cake-mode filtration process tends to require high operating pressures to press the melt through the dense and accumulated cake layer, and in the case of lack of sufficient pressure, even filter clogging can occur [167]. In the case of an aluminum melt, whose inclusions are very fine, i.e. smaller than the pores of the filter, the removal of the inclusions will take place by the deep-bed filtration mode, see Fig. 10c. That is the established filtration mode for NMIs removal from molten aluminum [168, 169], which acts based on two primary principles as shown in Fig. 11: (1) due to the inherently high surface area and narrow course of the filter, the particles collide with the pore walls on their way through the inside of the filter pores and adhere to them; (2) as inclusions continuously attach to the pore walls, inclusion bridges are progressively formed within the pore channels. These bridges further enhance the filtration efficiency by creating additional barriers, effectively sieving out more inclusions from the melt and improving overall purification rate [166].

The efficiency of the filtration process is highly influenced by various factors including the physicochemical properties of inclusions such as size, concentration, and nature of inclusion, as well as the properties of filters such as filter surface area, pore size, surface wettability and filter roughness. In addition, the fluid and process parameters such as the filtration speed, the presence of grain refiners, and hydrodynamics of the melt also influence the filtration performance [170–173]. The process of transporting particles with the melt to the surface or interior pores of filter also plays a critical role in the efficiency of deep-bed filtration, which is controlled by sedimentation, Brownian motion, fluid flow, inclusion collision or attachment to the filter walls [162, 174].

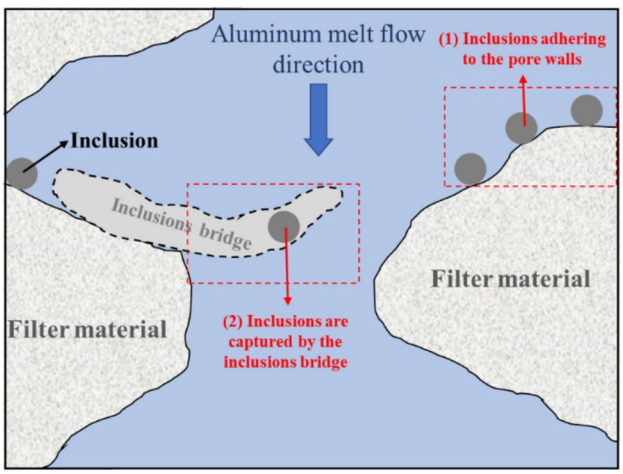

Figure 11 The fundamental mechanism of inclusions removal by deep-bed filtration [166], modified.

Scholars and industry agree that filters with smaller pore size (larger ppi number) have higher filtration efficiency, while inclusion removal decreases as the size of the inclusions decreases, [166, 175–177]. The 30-ppi filter almost completely removed inclusions larger than 125 μm and removed 85% of 5 μm inclusions, though small inclusions (< 5 μm) were hard to filter out [166]. Inclusion particles with smaller shape factor are easier to be removed by filtration [178]. However, small-pore sized filters have some issues such as short lifetime due to their extreme susceptibility to blockage by inclusions and the need to overcome a high pressure drop across the filter. The pore density of CFFs for industrial aluminum filtration typically ranges from 20 to 70 ppi, of which filters with 50–70 ppi are mainly used for the production of high-quality products [179]. The concentration of NMIs also has the effect of filtration efficiency. It has been demonstrated that reducing the concentration of SiC particles from 20 wt. % to 5 wt. % increased the filtration efficiency to more than 90% [180].

The addition of grain refiners to the molten aluminum, such as Al-3%Ti-1%B, Al-5%Ti-1%B and Al-3%Ti-0.15%C (e.g., 2.0 kg/tonne of Al) can reduce the filtration efficiency of ceramic foam filters (CFF), especially during the removal of oxide films [172, 181–184]. The degradation of filtration performance of the filters by grain refiners is due to the strong adherence between TiB_2, exemplary a very common grain refiner, to the oxide films in the melt. The attachment and agglomeration of heavy grain refiner particles onto light oxide films counteracts the gravitational number of oxide films and disrupt the formation of oxide inclusions bridges, making them difficult to be filtrated by CFF [181, 182]. The gravitational number, which quantifies the influence of gravity on inclusions, is primarily determined by the density difference

between the inclusion and the molten melt. As demonstrated by a 2D lattice-Boltzmann model calculation, this parameter also plays a critical role in the filtration efficiency [185]. Specifically, inclusions with a higher density than the melt exhibit a large positive gravitational number and tend to settle easily on the filter pore walls, facilitating their removal. In contrast, inclusions with a lower density than the melt have a large negative gravitational number and tend to float toward the melt surface. When the gravity number is high (large positive value) or low (large negative value), i.e. the inclusion density differs substantially from that of the melt, the filtration efficiency can be increased. When the gravity number of the inclusions is close to zero, i.e. the density is similar to the melt, the filtration efficiency decreases [182]. Instone et al. [186, 187] addressed the problems associated with the addition of grain refiners by developing the XC filter, which consists of three chambers with a ceramic foam filter in the first chamber, grain refiner addition in the second chamber and a small bed filter in the third chamber. The results of industrial casting trial proved that the XC filter achieved a high removal efficiency of 97% for inclusions larger than 50 μm, demonstrating its suitability for removing NMIs in industrial applications [188].

The hydrodynamics of the melt is also one of the most responsible factors for the filtration efficiency. Various studies have demonstrated that an appropriate reduction in the velocity of the melt or Reynolds number of the melt can effectively increase the filtration efficiency [166, 168, 178, 189]. In the Al-TiB_2 system, as the melt interstitial velocity, i.e. melt velocity inside the filter bed, increased from 0.2 cm/s to 0.5 cm/s, the removal efficiency of TiB_2 inclusions sharply reduced from as high as 70% to about 10%. [168].

The chemical and physical properties of the filter surface play a crucial role in influencing the filtration efficiency as well. Multiple functional coatings on filters have been developed to improve the filtration performance. Voigt et al. [170] successfully prepared five filters with different surface chemistry and coated by five different oxide surface materials like Al_2O_3, spinel ($MgAl_2O_4$), mullite ($Al_6Si_2O_{13}$), TiO_2, and SiO_2, on the alumina skeleton. Among them, the filters coated with spinel as well as Al_2O_3 achieved the highest NMIs separation efficiencies (90%) while the bigger sized inclusions ($d > 90$ μm) were completely removed [190]. To further investigate the effect of filter surface quality on the filtration behavior, ceramic foam filters containing Al_2O_3 nanocoating were prepared [172]. It was concluded that the Al_2O_3 nano-coating of such filters would not result in any improvement in filtration efficiencies [169, 171]. The contact angle between the molten melt and the filter material, i.e. wettability, which was caused by the difference in surface energy between the nanocoating and the reference material had no significant effect on the filtration efficiencies. In contrast, the surface roughness of the filter plays a critical role in determining filtration efficiencies [191, 192]. Compared to Al_2O_3 reference filter, Al_2O_3-C filter coated by the combined dip-spin technology had a better filtration performance, probably due to the presence of a Al_4O_4C-layer with a thickness between 10 μm up to 50 μm between the Al melt and Al_2O_3-C coating [193]. The uniform and tightly coated flux (e.g., 45% NaCl, 45%KCl, and 5% LaF_3) on the filter wall surface of the flux composite filter can facilitate the adsorption of inclusions [194].

As a summary, filtration technique, easily being integrated into continuous casting, is an effective and environmentally friendly method for removing nonmetallic inclusions from Al melt, especially for the production of high-quality Al alloys. However, filters accumulate inclusions during the filtration process leading to higher penetration resistance or even clogging, which reduces filtration efficiency and increases operating costs to replace the filter [180]. Multi-stage and multi-media filtration platforms have been therefore designed to combine multiple filters in a synergistic effect to significantly improve filtration performance and facilitate superior control of inclusion quantity, thus optimizing the conventional "inclusion removal-continuous casting" process widely employed in large-scale aluminum industries [195, 196].

Supergravity-enhanced separation

The relative motion due to the phase density difference ($\Delta\rho$) is a driving force of phase separation in metallurgical processes, e.g., the removal of NMIs from Al melts by sedimentation process, while the increase of the gravity coefficient intensifies the relative motion between phases and significantly enhances the mass transfer and phase. In recent years, the supergravity technology has been extensively investigated in the field of the melt and metallurgical purification due to its ability to strength the mass transfer and promote

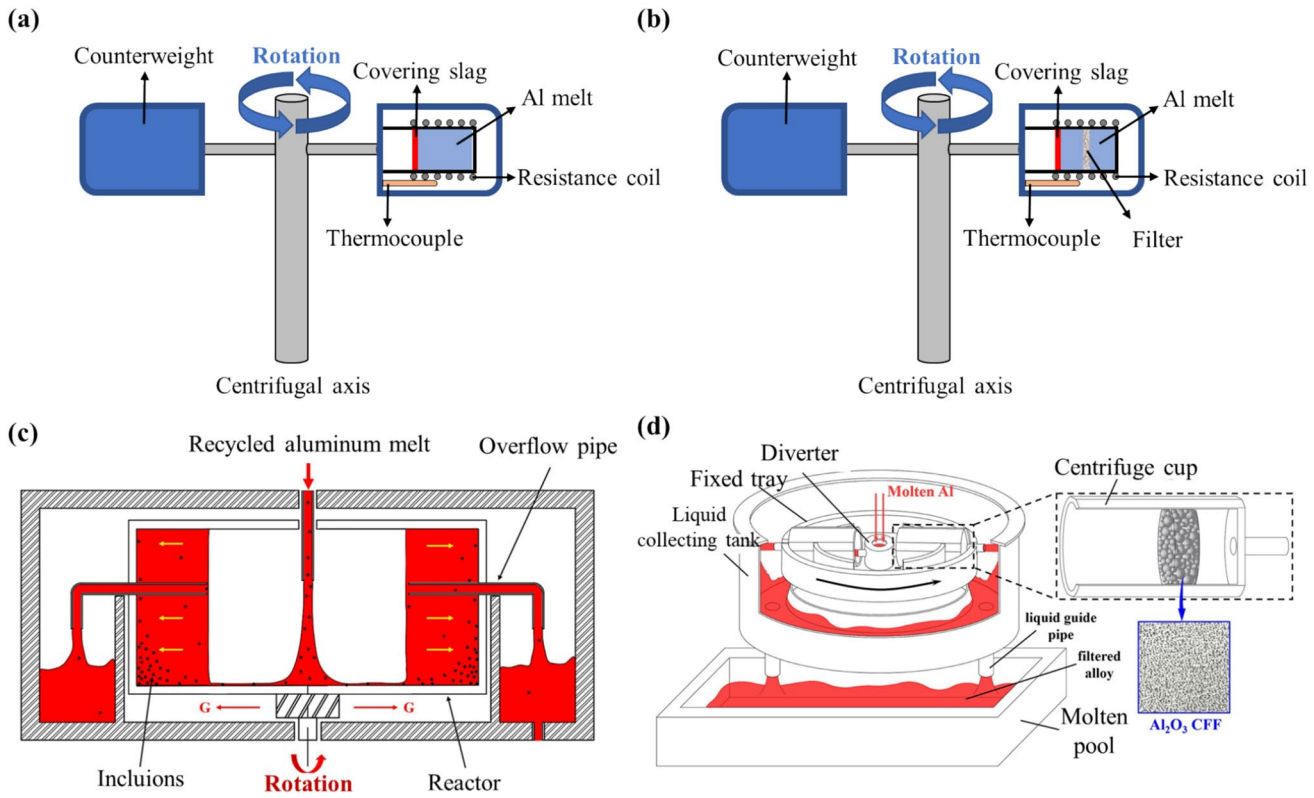

Figure 12 The schematic diagram of different kinds of experimental apparatus with supergravity field: **a** rotary centrifugal apparatus without filter [198], modified, **b** rotary centrifugal filtration apparatus with filter [199], modified, **c** overflow-type supergravity reactor [200], **d** continuous centrifugal filtration device [201].

the phase separation [197]. This field is normally achieved by applying high gravitational accelerations generated through the rotation of a centrifugal system [198–201]. Figure 12 illustrates various experimental apparatus used for the removal of NMIs under the supergravity field.

The gravity coefficient (G) is defined as the ratio of the super-gravitational acceleration to normal-gravitational acceleration (g), as expressed in Eq. [6]: [198]

$$G = \frac{\sqrt{g^2 + (\mathrm{r}w^2)^2}}{\mathrm{g}} = \frac{\sqrt{g^2 + (\frac{N^2\pi^2 r}{900})^2}}{\mathrm{g}} \quad (6)$$

where G is the gravity coefficient, ω (rad/s) is the angular velocity, N (r/min) is the rotating speed of the centrifugal, r (m) is the distance from the centrifugal axis to the center of the sample; and g (9.8 m/s^2) is the normal-gravitational acceleration. When N = 0 r/min, G = 1.

Song et al. [198, 202] demonstrated that the separation efficiency of inclusions increased rapidly with the increase of gravity coefficient, separation time, and melt temperature. At a gravity coefficient of 500 and a melt temperature of 1023 K, the $MgAl_2O_4$ inclusions were collected at the bottom of the specimen with a separation efficiency of 90% after two minutes by the rotary centrifugal apparatus as shown in Fig. 12a [202]. Wang et al. employed a combination of numerical and physical simulations to study the continuous separation process of inclusions from aluminum melt in an overflow-type supergravity reactor as show in Fig. 12c [200]. The results showed that the separation efficiency of 18 μm Al_2O_3 inclusions could be close to 100%.

The combination of supergravity with filtration technology, known as "supergravity filtration technology", can effectively overcome the strong seepage resistance (pressure drop) of filters with fine-pore filter medium (high ppi) [199]. A schematic diagram of rotary centrifugal filtration apparatus with filter is shown in Fig. 12b. After supergravity filtration, the sample can be automatically divided into the upper layer of residue and the lower layer of purified aluminum. As shown in Fig. 13, the removal efficiency

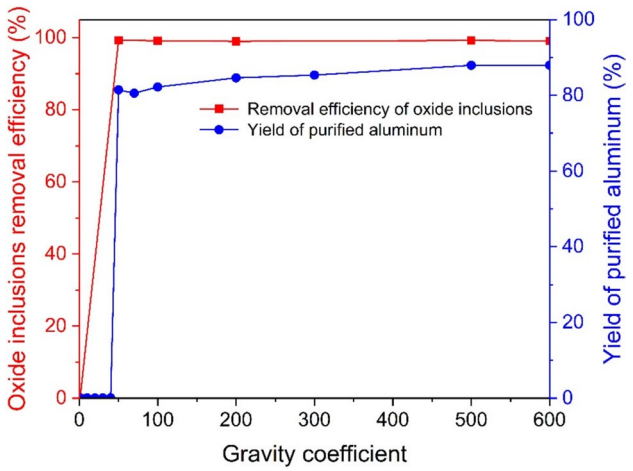

Figure 13 Removal efficiency of oxide inclusions and yield of purified aluminum with different gravity coefficients after supergravity filtration at t = 2 min and T = 700 °C [199], modified.

of $MgAl_2O_4$ spinel inclusions can achieve around 99% after a supergravity filtration time of 2 min at a gravity coefficient G ≥ 50 and melt temperature T = 700 °C, and the yield of purified aluminum reached 92.1% under G = 600, t = 2 min, and T = 700 °C [199]. Sun et al. [201] conducted industrial-scale experiments on continuous recovery of Al–Mg-Si alloy scrap utilizing a continuous centrifugal filtration device as shown in Fig. 12d, thus enabling continuous recovery of standard wrought alloys.

Compared to regular sedimentation process, supergravity technology overcomes the limitations of sedimentation process, which relies on a slower natural settling process, has low NMIs removal efficiency and is less effective at removing finer inclusions or those with low density differences relative to the melt. However, the process requires specialized centrifugal devices, which increases the equipment, operating as well as maintenance costs. Therefore, this technology is currently only applied in the laboratory and pilot scale stage. A full-scale industrial application needs still further research and developments.

Conclusions and future trends

Non-metallic inclusions in aluminum alloys negatively affect mechanical properties, such as strength, ductility, and fatigue resistance, while also degrading surface quality and increasing the risk of defects during casting and forming and decreasing corrosion resistance, ultimately deteriorating overall Al alloy performance. It has been recognized that the effective removal of non-metallic inclusions is an important aspect to ensure and enhance the quality of aluminum alloy products, making this a widely studied and highly relevant topic in the field of aluminum metallurgy. This paper systematically reviews the current research status of non-metallic inclusions removal techniques, including their principles, influencing factors, advantages and disadvantages.

As different processes have their own limitations, the appropriate purification technologies for aluminum melts will be selected based on the different demands, types of alloys and applications. Salt fluxing technique is widely used for processing contaminated or oxidized scrap, effectively promoting metal recovery, though it struggles with fine inclusions and raises environmental concerns. Sedimentation technique offers a low-cost solution for removing large, dense inclusions but is less effective for fine NMIs or NMIs with low densities difference to the melt. Gas purging technique facilitates continuous removal of hydrogen and inclusions. However, its efficiency diminishes for ultrafine NMIs and may introduce secondary contaminants if not carefully controlled. Electromagnetic separation technique provides rapid, contact-free, and highly efficient removal of micron-sized NMIs but faces limitations due to the skin effect and high costs. Filtration technique remains a key method in high-quality Al alloy production, especially when enhanced through multi-stage and multi-media systems. However, it suffers from filter clogging, which reduces filtration performance and increases operational costs. Supergravity-enhanced separation technology significantly improves the removal efficiency of fine inclusions or those with low density differences relative to the melt compared to conventional sedimentation process, but its industrial application is currently limited by the high cost and complexity of specialized centrifugal equipment. In many cases, the combination of multiple techniques is often used to achieve an optimum purification efficiency.

In general, extensive studies have been carried out on the effects of non-metallic inclusions on Al products and processing, as well as the NMIs removal techniques. By summarizing the current challenges in removing non-metallic inclusions from aluminum, the following outlooks are proposed for future research and development in this field:

1) To optimize the process parameters, and integrate multiple techniques based on the existing processes to develop more economical and efficient purification techniques.
2) In view of the limitations of the current process to remove submicron non-metallic inclusions, future research should focus on the improvement and development of novel purification techniques to achieve more comprehensive and effective removal of fine inclusions.
3) As the aluminum industries are in the direction of green transformation, there is a growing requirement to improve the process to develop non-toxic and non-polluting purification techniques, reduce the comprehensive energy consumption of the processes, and explore the waste treatment and recycling technology to ultimately achieve the goal of sustainable development.

Acknowledgements

The authors would like to thank China Scholarship Council (CSC) for the financial support of the PhD candidate Mr. Bo Yang.

Author contributions

Conceptualization, B.Y and S.F..; investigation, B.Y.; writing—original draft preparation, B.Y.; writing—review and editing, S.F.; supervision, S.F.; project administration, S.F.; principal investigator, B.F.; All authors have read and agreed to the published version of the manuscript.

Funding

Open Access funding enabled and organized by Projekt DEAL.

Declarations

Conflict of interest The authors declare no conflicts of interest.

Ethical approval Not applicable.

References

[1] International Aluminium Institute. Primary aliminium production. https://international-aluminium.org/statistics/primary-aluminium-production (Accessed on 2025–05–20)
[2] Zhan H, Zeng G, Wang Q et al (2023) Unified casting (UniCast) aluminum alloy—a sustainable and low-carbon materials solution for vehicle lightweighting. J Mater Sci Technol 154:251–268. https://doi.org/10.1016/j.jmst.2023.02.003
[3] Martinez R, Guillot I, Massinon D (2019) New heat treatment to improve the mechanical properties of low copper aluminum primary foundry alloy. Mater Sci Eng A 755:158–165. https://doi.org/10.1016/j.msea.2019.04.001
[4] Knabner D, Suchý L, Radtke S, Leidich E, Hasse A (2024) Fretting fatigue of cast iron and aluminium—a strength assessment method based on a worst-case assumption. Int J Fatigue 182:108209. https://doi.org/10.1016/j.ijfatigue.2024.108209
[5] Abuserwal AF, Elizondo Luna EM, Goodall R, Woolley R (2017) The effective thermal conductivity of open cell replicated aluminium metal sponges. Int J Heat Mass Transfer 108:1439–1448. https://doi.org/10.1016/j.ijheatmasstransfer.2017.01.023
[6] Liang Y, Li G, Liu L et al (2023) Corrosion behavior of Al-6.8Zn-2.2Mg-Sc-Zr alloy with high resistance to intergranular corrosion. J Mater Sci Technol 24:7552–7569. https://doi.org/10.1016/j.jmrt.2023.05.017
[7] Mishra RR, Sharma AK (2016) On mechanism of in-situ microwave casting of aluminium alloy 7039 and cast microstructure. Mater Des 112:97–106. https://doi.org/10.1016/j.matdes.2016.09.041
[8] Li SS, Yue X, Li QY et al (2023) Development and applications of aluminum alloys for aerospace industry. J Mater Sci Technol 27:944–983. https://doi.org/10.1016/j.jmrt.2023.09.274
[9] Selvamani ST (2021) MicrostructureSS and stress corrosion behaviour of CMT welded AA6061 T-6 aluminium alloy joints. J Mater Sci Technol 15:315–326. https://doi.org/10.1016/j.jmrt.2021.08.005

[10] Georgantzia E, Gkantou M, Kamaris GS (2021) Aluminium alloys as structural material: a review of research. Eng Struct 227:111372. https://doi.org/10.1016/j.engstruct.2020.111372

[11] Zhang L, Lv XW, Torgerson AT, Long M (2011) Removal of impurity elements from molten aluminum: a review. Miner Process Extr Metall Rev 32:150–228. https://doi.org/10.1080/08827508.2010.483396

[12] Hudson SW, Apelian D (2016) Inclusion detection in molten aluminum: current art and new avenues for in situ analysis. Miner Process Extr Metall Rev 10:289–305. https://doi.org/10.1007/s40962-016-0030-x

[13] Hedjazi D, Bennett GHJ, Kondic V (1976) Effects of nonmetallic inclusions on tensile properties of an Al-4-5Cu-1.5Mg alloy. Met Technol 3B:537–541. https://doi.org/10.1179/030716976803392132

[14] Murakami Y (2019) Metal fatigue: effects of small defects and nonmetallic inclusions. Academic Press. https://doi.org/10.1016/B978-0-12-813876-2.00006-6

[15] Zerbst U, Madia M, Klinger C, Bettge D, Murakami Y (2019) Defects as a root cause of fatigue failure of metallic components. II: non-metallic inclusions. Eng Fail Anal 98:228–239. https://doi.org/10.1016/j.engfailanal.2019.01.054

[16] Bowles CQ, Schijve J (1973) The role of inclusions in fatigue crack initiation in an aluminum alloy. Int J Fract 9:171–179. https://doi.org/10.1007/BF00041859

[17] Liu L, Samuel FH (1998) Effect of inclusions on the tensile properties of Al-7% Si-0.35% Mg (A356.2) aluminium casting alloy. J Mater Sci 33:2269–2281. https://doi.org/10.1023/A:1004331219406

[18] Chiesa F, Levasseur D, Morin G, Duchesne B (2016) Effect of inclusions on the tensile properties inside a LPPM A356 casting. Miner Process Extr Metall Rev 10:216–223. https://doi.org/10.1007/s40962-016-0029-3

[19] Keles O, Dundar M (2007) Aluminum foil: its typical quality problems and their causes. J Mater Process Technol 186:125–137. https://doi.org/10.1016/j.jmatprotec.2006.12.027

[20] Rezaul Karim M, Kadau K, Narasimhachary S et al (2021) Crack nucleation from non-metallic inclusions in aluminum alloys described by peridynamics simulations. Int J Fatigue 153:106475. https://doi.org/10.1016/j.ijfatigue.2021.106475

[21] Di Sabatino M, Arnberg L, Apelian D (2008) Progress on the understanding of fluidity of aluminium foundry alloys. Miner Process Extr Metall Rev 2:17–27. https://doi.org/10.1007/BF03355430

[22] Kwon YD, Lee ZH (2003) The effect of grain refining and oxide inclusion on the fluidity of Al-4.5Cu-0.6Mn and A356 alloys. Mater Sci Eng A 360:372–376. https://doi.org/10.1016/S0921-5093(03)00504-5

[23] Rødseth J, Rasch B, Lund O, Thonstad J (2002) Solubility of carbon in aluminium and its effect upon the casting process. Light metals: Proceedings of Sessions, TMS annual meeting (Warrendale, Pennsylvania): pp. 883–887

[24] Anyalebechi PN (2013) Hydrogen-induced gas porosity formation in Al-4.5 wt% Cu-1.4 wt% Mg alloy. J Mater Sci 48:5342–5353. https://doi.org/10.1007/s10853-013-7329-2

[25] Chen XG, Gruzleski JE (1996) Influence of melt cleanliness on pore formation in aluminium-silicon alloys. Int J Cast Met Res 9:17–26. https://doi.org/10.1080/13640461.1996.11819640

[26] Tian C, Law J, van der Touw J et al (2002) Effect of melt cleanliness on the formation of porosity defects in automotive aluminium high pressure die castings. J Mater Process Technol 122:82–93. https://doi.org/10.1016/S0924-0136(01)01229-8

[27] Ravi KR, Pillai RM, Amaranathan KR, Pai BC, Chakraborty M (2008) Fluidity of aluminum alloys and composites: a review. J Alloys Compd 456:201–210. https://doi.org/10.1016/j.jallcom.2007.02.038

[28] Zhang Y, Li R, Li X et al (2018) Possible effects and mechanisms of ultrasonic cavitation on oxide inclusions during direct-chill casting of an Al alloy. Metals 8:814. https://doi.org/10.3390/met8100814

[29] Ma Z, Samuel AM, Samuel FH, Doty HW, Valtierra S (2008) A study of tensile properties in Al-Si-Cu and Al-Si-Mg alloys: effect of β-iron intermetallics and porosity. Mater Sci Eng A 490:36–51. https://doi.org/10.1016/j.msea.2008.01.028

[30] Campbell J (2016) The consolidation of metals: the origin of bifilms. J Mater Sci 51:96–106. https://doi.org/10.1007/s10853-015-9399-9

[31] Campbell J (2019) Update on bifilms—the fundamental defect in metals. In: Tiryakioğlu M, Griffiths W, Jolly M (eds) Shape casting. The minerals, metals & materials series. Springer, Cham, pp 3–15. https://doi.org/10.1007/978-3-030-06034-3_1

[32] Uludağ M, Çetin R, Dişpinar D, Tiryakioğlu M (2018) On the interpretation of melt quality assessment of A356 aluminum alloy by the reduced pressure test: the bifilm index and its physical meaning. Miner Process Extr Metall Rev 12:853–860. https://doi.org/10.1007/s40962-018-0217-4

[33] Costa e Silva ALVd (2019) The effects of non-metallic inclusions on properties relevant to the performance of steel in structural and mechanical applications. J Mater Res Technol 8:2408–2422. https://doi.org/10.1016/j.jmrt.2019.01.009

[34] Chan KS (2010) Roles of microstructure in fatigue crack initiation. Int J Fatigue 32:1428–1447. https://doi.org/10.1016/j.ijfatigue.2009.10.005

[35] Knott JF, King JE (1991) Fatigue in metallic alloys containing non-metallic particles. Mater Des 12:67–74. https://doi.org/10.1016/0261-3069(91)90107-F

[36] Du S, Zhang S, Wang M et al (2024) High-temperature heat treatment attenuating the influence of micron-sized inclusions on the microstructure and properties of recycled Al-Zn-Mg-Cu alloy sheet. J Mater Sci Technol 30:4147–4158. https://doi.org/10.1016/j.jmrt.2024.04.092

[37] Yan W, Fu G, Chen H, Chen G (2012) Effects of oxide inclusions on flow stress behavior of 1235 aluminum alloy during hot compression. J Mater Eng Perform 21:2203–2206. https://doi.org/10.1007/s11665-012-0152-0

[38] Yan WD, Fu GS, Lai WQ et al (2021) Effects of oxide inclusions on texture of 1235 Al-alloy after deformation. Mater Sci Forum 1023:53–59. https://doi.org/10.4028/www.scientific.net/MSF.1023.53

[39] You K, Rao L, Wen J, Dong Y (2022) Mechanism for the induction and enhancement of inclusions on crack source and simulation analysis for hot tearing tendency of aluminum alloy. Modell Simul Mater Sci Eng 30:085002. https://doi.org/10.1088/1361-651X/ac9693

[40] Akhtar S, Dispinar D, Arnberg L, Di Sabatino M (2009) Effect of hydrogen content, melt cleanliness and solidification conditions on tensile properties of A356 alloy. Int J Cast Met Res 22:22–25. https://doi.org/10.1179/136404609X367245

[41] Fankhänel B, Hubálková J, Aneziris CG, Stelter M, Charitos A (2022) Influencing the hydrogen porosity in aluminum casting by (re)active filter materials. Adv Eng Mater 24:2100579. https://doi.org/10.1002/adem.202100579

[42] Majidi O, Shabestari SG, Aboutalebi MR (2007) Study of fluxing temperature in molten aluminum refining process. J Mater Process Technol 182:450–455. https://doi.org/10.1016/j.jmatprotec.2006.09.003

[43] Dispinar D, Akhtar S, Nordmark A, Di Sabatino M, Arnberg L (2010) Degassing, hydrogen and porosity phenomena in A356. Mater Sci Eng A 527:3719–3725. https://doi.org/10.1016/j.msea.2010.01.088

[44] Griffiths WD, Raiszadeh R (2009) Hydrogen, porosity and oxide film defects in liquid Al. J Mater Sci 44:3402–3407. https://doi.org/10.1007/s10853-009-3450-7

[45] Tiryakioğlu M (2020) The effect of hydrogen on pore formation in aluminum alloy castings: myth versus reality. Metals 10:368. https://doi.org/10.3390/met10030368

[46] Tiryakioğlu M (2019) The myth of hydrogen pores in aluminum castings. In: Tiryakioğlu M, Griffiths W, Jolly M (eds) Shape casting. The minerals, metals & materials series. Springer, Cham, pp 143–150. https://doi.org/10.1007/978-3-030-06034-3_14

[47] Chen YJ (2010) Ultrasonic evaluation of the quality of A356.2 alloy by fluxing treatment. Mater Trans 51:803–809. https://doi.org/10.2320/matertrans.M2009416

[48] Milani V, Timelli G (2023) Solid salt fluxes for molten aluminum processing—a review. Metals 13:832. https://doi.org/10.3390/met13050832

[49] Utigard TA (1998) The properties and uses of fluxes in molten aluminum processing. JOM 50:38–43. https://doi.org/10.1007/s11837-998-0285-7

[50] Utigard TA, Roy RR, Friesen K (2001) The roles of molten salts in the treatment of aluminum. Can Metall Q 40:327–334. https://doi.org/10.1179/cmq.2001.40.3.327

[51] Utigard TA, Roy RR, Friesen K (2001) Properties of fluxes used in molten aluminium processing. High Temp Mater Processes (London) 20:303–308. https://doi.org/10.1515/HTMP.2001.20.3-4.303

[52] Wan B, Li W, Liu F et al (2020) Determination of fluoride component in the multifunctional refining flux used for recycling aluminum scrap. J Mater Sci Technol 9:3447–3459. https://doi.org/10.1016/j.jmrt.2020.01.082

[53] Li C, Li JG, Mao YZ, Ji JC (2017) Mechanism to remove oxide inclusions from molten aluminum by solid fluxes refining method. China Foundry 14:233–243. https://doi.org/10.1007/s41230-017-7005-2

[54] Shi M, Li Y (2023) Performance improvement in aluminum alloy treated by salt flux with different fluorides. J Mater Eng Perform 32:3065–3072. https://doi.org/10.1007/s11665-022-07306-1

[55] Vijayan V, Shetty A, Pawan Kumar B, Hiremath S, Kumar P, Vishwanatha HM (2023) A comprehensive analysis of cooling curves, fluidity, inclusions, porosity, and microstructure of NaCl-KCl-NaF flux treated Al-12Si alloy. Mater Res Express 10:126506. https://doi.org/10.1088/2053-1591/ad135b

[56] Roy RR, Sahai Y (1997) Coalescence behavior of aluminum alloy drops in molten salts. Mater Trans, JIM 38:995–1003. https://doi.org/10.2320/matertrans1989.38.995

[57] Roy RR, Utigard TA (1998) Interfacial tension between aluminum and NaCl-KCl-based salt systems. Metall Mater Trans B 29:821–827. https://doi.org/10.1007/s11663-998-0141-8

[58] Roy RR, Sahai Y (1997) Interfacial tension between aluminum alloy and molten salt flux. Mater Trans, JIM 38:546–552. https://doi.org/10.2320/matertrans1989.38.546

[59] Gallo R (2017) I have inclusions! Get me the cheapest and best Flux for cleaning my melt'-Is this the best driven, cost saving approach by a foundry?. Proceedings of the 121st Metalcasting Congress of the American Foundry Society.

[60] Masson DB, Taghiei MM (1989) Interfacial reactions between aluminum alloys and salt flux during melting. Mater Trans, JIM 30:411–422. https://doi.org/10.2320/matertrans1989.30.411

[61] Tenorio JAS, Carboni MC, Espinosa DCR (2001) Recycling of aluminum–effect of fluoride additions on the salt viscosity and on the alumina dissolution. J Light Met 1:195–198. https://doi.org/10.1016/S1471-5317(01)00013-X

[62] Xiao Y, Reuter MA (2002) Recycling of distributed aluminium turning scrap. Miner Eng 15:963–970. https://doi.org/10.1016/S0892-6875(02)00137-1

[63] Arianpour F, Arianpour AÇ, Aali B (2021) Characterization and properties of sodium hexa-fluorosilicate and its potential application in the production of sodium fluoride. SILICON 13:4381–4389. https://doi.org/10.1007/s12633-020-00755-0

[64] Huang C, Liu Z, Huang J, Liu Q, Li J (2021) Effect of sodium-containing fluxes on the residual sodium content and distribution in Al–Mg alloys. Metals 11:1591. https://doi.org/10.3390/met11101591

[65] Zhang S, Han Q, Liu ZK (2007) Fundamental understanding of Na-induced high temperature embrittlement in Al-Mg alloys. Philos Mag 87:147–157. https://doi.org/10.1080/14786430600941587

[66] Talbot DEJ, Ransley CE (1977) The addition of bismuth to aluminum-magnesium alloys to prevent embrittlement by sodium. Metall Trans A 8:1149–1154. https://doi.org/10.1007/BF02667400

[67] Zhang G, Lu W, Wu X et al (2023) A new strategy on designing fluxes for aluminum alloy melt refinement. Materials 16:2322. https://doi.org/10.3390/ma16062322

[68] Campbell J (2015) Chapter 2: Entrainment. In: Complete casting handbook: metal casting processes, metallurgy, techniques and design. Butterworth-Heinemann, Bosten

[69] Smirnov O, Fikssen V, Kukhar V et al (2025) Correction: thin-walled aluminium waste remelting in circulation circuit with magnetodynamic pump. J Mater Sci 60:4946–4947. https://doi.org/10.1007/s10853-025-10737-5

[70] Amini Mashhadi H, Moloodi A, Golestanipour M, Karimi EZV (2009) Recycling of aluminium alloy turning scrap via cold pressing and melting with salt flux. J Mater Process Technol 209:3138–3142. https://doi.org/10.1016/j.jmatprotec.2008.07.020

[71] Vallejo-Olivares A, Philipson H, Gökelma M et al (2021) Compaction of aluminium foil and its effect on oxidation and recycling yield. In: Perander L (ed) Light metals 2021 The minerals, metals & materials series. Springer, Cham, pp 735–741. https://doi.org/10.1007/978-3-030-65396-5_96

[72] Gökelma M, Vallejo-Olivares A, Tranell G (2021) Characteristic properties and recyclability of the aluminium fraction of MSWI bottom ash. Waste Manage (Oxford) 130:65–73. https://doi.org/10.1016/j.wasman.2021.05.012

[73] Gökelma M, Einarsrud KE, Tranell G, Friedrich B (2020) Shape factor effect on inclusion sedimentation in aluminum melts. Metall Mater Trans B 51:850–860. https://doi.org/10.1007/s11663-020-01769-0

[74] Sztur C, Balestreri F, Meyer JL, Hannart B (2016) Settling of inclusions in holding furnaces: modeling and experimental results. In: Grandfield JF, Eskin DG (eds) Essential readings in light metals. Springer, Cham. https://doi.org/10.1007/978-3-319-48228-6_14

[75] Martin JP, Dubé G, Frayce D, Guthrie R (2016) Settling phenomena in casting furnaces: a fundamental and experimental investigation. In: Grandfield JF, Eskin DG (eds) Essential readings in light metals. Springer, Cham. https://doi.org/10.1007/978-3-319-48228-6_15

[76] Gökelma M, Le Brun P, Dang T et al (2016) Assessment of settling behavior of particles with different shape factors by LiMCA data analysis. In: Williams E (ed) Light metals 2016.

Springer, Cham. https://doi.org/10.1007/978-3-319-48251-4_143
[77] Badowski M, Gökelma M, Morscheiser J, Dang T, Le Brun P, Tewes S (2016) Study of Particle Settling and Sedimentation in a Crucible Furnace. In: Hyland M (ed) Light metals 2015. Springer, Cham. https://doi.org/10.1007/978-3-319-48248-4_162
[78] Kolsgaard A, Brusethaug S (1993) Settling of SiC particles in an AlSi7Mg melt. Mater Sci Eng A 173:213–219. https://doi.org/10.1016/0921-5093(93)90218-4
[79] Ourdjini A, Chew KC, Khoo BT (2001) Settling of silicon carbide particles in cast metal matrix composites. J Mater Process Technol 116:72–76. https://doi.org/10.1016/S0924-0136(01)00843-3
[80] Heidary DSB, Akhlaghi F (2011) Theoretical and experimental study on settling of SiC particles in composite slurries of aluminum A356/SiC. Acta Mater 59:4556–4568. https://doi.org/10.1016/j.actamat.2011.03.077
[81] Schaffer PL, Dahle AK (2005) Settling behaviour of different grain refiners in aluminium. Mater Sci Eng A 413–414:373–378. https://doi.org/10.1016/j.msea.2005.08.202
[82] Gyarmati G, Bogoly L, Stawarz M et al (2022) Grain refiner settling and its effect on the melt quality of aluminum casting alloys. Materials 15:7679. https://doi.org/10.3390/ma15217679
[83] Gazanion F, Chen XG, Dupuis C (2002) Studies on the sedimentation and agglomeration behavior of Al-Ti-B and Al-Ti-C grain refiners. Mater Sci Forum 396–402:45–52. https://doi.org/10.4028/www.scientific.net/MSF.396-402.45
[84] Ahmadi G (2004) Particle transport, deposition and removal. Proc ME 437: 1028À1040.
[85] Bagheri G, Bonadonna C (2016) On the drag of freely falling non-spherical particles. Powder Technol 301:526–544. https://doi.org/10.1016/j.powtec.2016.06.015
[86] Yue Q, Zou ZS, Hou QF (2010) Aggregation kinetics of inclusions in swirling flow tundish for continuous casting. J Iron Steel Res Int 17:6–10. https://doi.org/10.1016/S1006-706X(10)60091-X
[87] Alipchenkov VM, Zaichik LI (2001) Particle collision rate in turbulent flow. Fluid Dyn 36:608–618. https://doi.org/10.1023/A:1012345714538
[88] Cournil M, Gruy F, Gardin P, Saint-Raymond H (2006) Modelling of solid particle aggregation dynamics in non-wetting liquid medium. Chem Eng Process 45:586–597. https://doi.org/10.1016/j.cep.2006.01.003
[89] Nakaoka T, Taniguchi S, Matsumoto K, Johansen ST (2001) Particle-size-grouping method of inclusion agglomeration and its application to water model experiments. ISIJ Int 41:1103–1111. https://doi.org/10.2355/isijinternational.41.1103
[90] Tian C, Irons GA, Wilkinson DS (1998) Monte carlo simulation of clustering of alumina particles in turbulent liquid aluminum. Metall Mater Trans B 29:785–791. https://doi.org/10.1007/s11663-998-0137-4
[91] Wang Q, Qi F, Li B, Tsukihashi F (2014) Behavior of nonmetallic inclusions in a continuous casting tundish with channel type induction heating. ISIJ Int 54:2796–2805. https://doi.org/10.2355/isijinternational.54.2796
[92] Irons GA, Owusu-Boahen K (1995) Settling and clustering of silicon carbide particles in aluminum metal matrix composites. Metall Mater Trans B 26:981–989. https://doi.org/10.1007/BF02654099
[93] Instone S, Buchholz A, Gruen GU (2008) Inclusion transport phenomena in casting furnaces. Light Metals 2008:811–816
[94] Takeo M (2000) Brownian motion of particles in concentrated suspensions. Appl Energy 67:61–89. https://doi.org/10.1016/S0306-2619(00)00007-6
[95] Assael MJ, Kakosimos K, Banish RM et al (2006) Reference data for the density and viscosity of liquid aluminum and liquid iron. J Phys Chem Ref Data 35:285–300. https://doi.org/10.1063/1.2149380
[96] Leroy C, Pignault G (1991) The use of rotating-impeller gas injection in aluminum processing. JOM 43:27–30. https://doi.org/10.1007/BF03222231
[97] Gómez ER, Zenit R, Rivera CG, Trápaga G, Ramírez-Argáez MA (2013) Physical modeling of fluid flow in ladles of aluminum equipped with impeller and gas purging for degassing. Metall Mater Trans B 44:974–983. https://doi.org/10.1007/s11663-013-9845-5
[98] Yang HL, He P, Zhai YC (2014) Removal behavior of inclusions in molten steel by bubble wake flow based on water model experiment. ISIJ Int 54:578–581. https://doi.org/10.2355/isijinternational.54.578
[99] Xu Y, Ersson M, Jönsson PG (2016) A numerical study about the influence of a bubble wake flow on the removal of inclusions. ISIJ Int 56:1982–1988. https://doi.org/10.2355/isijinternational.ISIJINT-2016-249
[100] Mirgaux O, Ablitzer D, Waz E, Bellot JP (2008) Removal of inclusions from molten aluminium by flotation in a stirred reactor: a mathematical model and a computer simulation. Int J Chem React Eng. https://doi.org/10.2202/1542-6580.1692
[101] Engh TA, Sigworth GK, Kvithyld A (2021) Chapter: 5 Removal of inclusions from melts. In: Engh TA, Sigworth GK, Kvithyld A (eds) Principles of metal refining and recycling. Oxford University Press, Oxford. https://doi.org/10.1093/oso/9780198811923.001.0001
[102] Warke VS, Shankar S, Makhlouf MM (2005) Mathematical modeling and computer simulation of molten aluminum cleansing by the rotating impeller degasser: part II removal of hydrogen gas and solid particles. J Mater Process Technol 168:119–126. https://doi.org/10.1016/j.jmatprotec.2004.10.016
[103] Zhang L, Taniguchi S (2000) Fundamentals of inclusion removal from liquid steel by bubble flotation. Int Mater Rev 45:59–82. https://doi.org/10.1179/095066000101528313
[104] Falsetti LOZ, Ferreira Muche DN, Santos Junior Td, Pandolfelli VC (2021) Thermodynamics of smart bubbles: the role of interfacial energies in porous ceramic production and non-metallic inclusion removal. Ceram Int 47:14216–14225. https://doi.org/10.1016/j.ceramint.2021.02.006
[105] Law BM, McBride SP, Wang JY et al (2017) Line tension and its influence on droplets and particles at surfaces. Prog Surf Sci 92:1–39. https://doi.org/10.1016/j.progsurf.2016.12.002
[106] McBride SP, Law BM (2012) Influence of line tension on spherical colloidal particles at liquid-vapor interfaces. Phys Rev Lett 109:196101. https://doi.org/10.1103/PhysRevLett.109.196101
[107] Falsetti LOZ, Delfos R, Charruault F, Luchini B, Van Der Plas D, Pandolfelli VC (2024) Wettability of non-metallic inclusions and its impact on bubble-induced flotation kinetics. Int J Appl Ceram Technol 21:3835–3841. https://doi.org/10.1111/ijac.14849
[108] Wang D, Liu Q (2021) Hydrodynamics of froth flotation and its effects on fine and ultrafine mineral particle flotation: a literature review. Miner Eng 173:107220. https://doi.org/10.1016/j.mineng.2021.107220
[109] Mostafaei M, Ghobadi M, Eisaabadi BG, Uludağ M, Tiryakioğlu M (2016) Evaluation of the effects of rotary degassing process variables on the quality of A357 aluminum alloy castings.

Metall Mater Trans B 47:3469–3475. https://doi.org/10.1007/s11663-016-0786-7
[110] Yamamoto T, Kato W, Komarov SV, Ishiwata Y (2019) Investigation on the surface vortex formation during Mechanical stirring with an axial-flow impeller used in an aluminum process. Metall Mater Trans B 50:2547–2556. https://doi.org/10.1007/s11663-019-01681-2
[111] Lee C, So T, Shin K (2016) Effect of gas bubbling filtration treatment on microporosity variation in A356 aluminium alloy. Acta Metallurgica Sinica (English Letters) 29:638–646. https://doi.org/10.1007/s40195-016-0434-x
[112] Wan B, Chen W, Mao M, Fu Z, Zhu D (2018) Numerical simulation of a stirring purifying technology for aluminum melt. J Mater Process Technol 251:330–342. https://doi.org/10.1016/j.jmatprotec.2017.09.001
[113] Chang S, Huang W, Zou Z, Li B, Guthrie RIL (2020) Motion behavior of micro-bubbles in a delta shape tundish using impact pad. Powder Technol 367:296–304. https://doi.org/10.1016/j.powtec.2020.03.051
[114] Maniruzzaman M, Makhlouf M (2002) Mathematical modeling and computer simulation of the rotating impeller particle flotation process: Part I. Fluid flow Metall Mater Trans B 33:297–303. https://doi.org/10.1007/s11663-002-0013-6
[115] Maniruzzaman M, Makhlouf M (2002) Mathematical modeling and computer simulation of the rotating impeller particle flotation process: part II particle agglomeration and flotation. Metall Mater Trans B 33:305–314. https://doi.org/10.1007/s11663-002-0014-5
[116] Warke VS, Tryggvason G, Makhlouf MM (2005) Mathematical modeling and computer simulation of molten metal cleansing by the rotating impeller degasser: part I fluid flow. J Mater Process Technol 168:112–118. https://doi.org/10.1016/j.jmatprotec.2004.10.017
[117] Li C, Gökelma M, Stets W, Friedrich B (2024) The separation behavior of TiB_2 during Cl_2-Free degassing treatment of 5083 aluminum melt. Metals 14:402. https://doi.org/10.3390/met14040402
[118] Chang S, Cao X, Hsin CH, Zou Z, Isac M, Guthrie RIL (2016) Removal of inclusions using micro-bubble Swarmss in a four-strand, full-scale, water model tundish. ISIJ Int 56:1188–1197. https://doi.org/10.2355/isijinternational.ISIJINT-2016-077
[119] Zhang S, Liu J, He Y et al (2023) Study of dispersed microbubbles and improved inclusion removal in Ruhrstahl-Heraeus (RH) refining with argon injection through down leg. Metall Mater Trans B 54:2347–2359. https://doi.org/10.1007/s11663-023-02836-y
[120] Tiwari R, Gonzalez-Morales D, Isac MM, Guthrie RIL (2024) A novel experimental set-up for generating microbubbles for the removal of inclusions from water and liquid metals. CIM Journal 15:21–32. https://doi.org/10.1080/19236026.2023.2255094
[121] Chang Z, Niu S, Shen Z, Zou L, Wang H (2023) Latest advances and progress in the microbubble flotation of fine minerals: microbubble preparation, equipment, and applications. Int J Min Met Mater 30:1244–1260. https://doi.org/10.1007/s12613-023-2615-8
[122] Saternus M, Merder T (2022) Physical modeling of the impeller construction impact on the aluminum refining process. Materials 15:575. https://doi.org/10.3390/ma15155273
[123] Yamamoto T, Suzuki A, Komarov SV, Ishiwata Y (2018) Investigation of impeller design and flow structures in mechanical stirring of molten aluminum. J Mater Process Technol 261:164–172. https://doi.org/10.1016/j.jmatprotec.2018.06.012
[124] Eckert CE, Walker NG (1992) Impeller for treating molten metals. United States Patent No. 5160693
[125] Cooper PV (2004) Molten metal degassing device and impellers therefor. United States Patent No. 6689310
[126] Grandfield J (2017) Developments in inclusion removal technology. In: Ratvik A (ed) Light metals 2017. The minerals, metals & materials series. Springer, Cham. https://doi.org/10.1007/978-3-319-51541-0_170
[127] Sigworth GK, Williams EM, Chesonis DC (2016) Gas fluxing of molten aluminum: an overview. In: Grandfield JF, Eskin DG (eds) Essential readings in light metals. Springer, Cham. https://doi.org/10.1007/978-3-319-48228-6_9
[128] Gökelma M, Storm Aarnæs T, Maier J et al (2021) Behavior of Al_4C_3 particles during flotation and sedimentation in aluminum melts. Metall Mater Trans B 52:743–754. https://doi.org/10.1007/s11663-020-02049-7
[129] Gyarmati G, Fegyverneki G, Tokár M, Mende T (2021) The effects of rotary degassing treatments on the melt quality of an Al-Si casting alloy. Miner Process Extr Metall Rev 15:141–151. https://doi.org/10.1007/s40962-020-00428-z
[130] Emley EF (1976) Cleansing and degassing of light metals. Met Technol 3:118–127. https://doi.org/10.1179/030716976803391403
[131] Gyarmati G, Pálóczi Á, Somfai D, Ferenczi T, Mende T, Kéri Z (2025) Analysis of different commercial solid fluxes used during the rotary degassing melt treatment of casting aluminum alloys. Metall Mater Trans B 56:782–797. https://doi.org/10.1007/s11663-024-03376-9
[132] Dispinar D, Campbell J (2011) Porosity, hydrogen and bifilm content in Al alloy castings. Mater Sci Eng A 528:3860–3865. https://doi.org/10.1016/j.msea.2011.01.084
[133] Gyarmati G, Vincze F, Fegyverneki G, Kéri Z, Mende T, Molnár D (2022) The effect of rotary degassing treatments with different purging gases on the double oxide- and nitride film content of liquid aluminum alloys. Metall Mater Trans B 53:1244–1257. https://doi.org/10.1007/s11663-021-02414-0
[134] Tremblay É, Maltais B (2017) The use of nitrogen to degas molten aluminium—Comparison of metallurgical results with argon and nitrogen used in an ACDtm. In: Ratvik A (ed) Light metals 2017. The minerals, metals & materials series. Springer, Cham. https://doi.org/10.1007/978-3-319-51541-0_176
[135] Zhang L, Wang S, Dong A, Gao J, Damoah LNW (2014) Application of electromagnetic (EM) separation technology to metal refining processes: a review. Metall Mater Trans B 45:2153–2185. https://doi.org/10.1007/s11663-014-0123-y
[136] Shu D, Li TX, Sun BD, Zhou YH, Wang J, Xu ZM (2000) Numerical calculation of the electromagnetic expulsive force upon nonmetallic inclusions in an aluminum melt: part I. Spherical particles Metall Mater Trans B 31:1527–1533. https://doi.org/10.1007/s11663-000-0037-8
[137] Reza Afshar M, Reza Aboutalebi M, Guthrie RIL, Isac M (2010) Modeling of electromagnetic separation of inclusions from molten metals. J Mater Process Technol 52:1107–1114. https://doi.org/10.1016/j.ijmecsci.2009.11.003
[138] Shimasaki SI, Takahashi K, Kanno Y, Taniguchi S (2016) Separation of inclusion particles from liquid metal by electromagnetic force. In: Weiland H, Rollett AD, Cassada WA (eds) ICAA13 Pittsburgh. Springer, Cham. https://doi.org/10.1007/978-3-319-48761-8_203
[139] Kolin A (1953) An electromagnetokinetic phenomenon involving migration of neutral particles. Science 117:134–137. https://doi.org/10.1126/science.117.3032.134

[140] Leenov D, Kolin A (1954) Theory of electromagnetophoresis. I. Magnetohydrodynamic forces experienced by spherical and symmetrically oriented cylindrical particles. J Chem Phys 22:683–688. https://doi.org/10.1063/1.1740149
[141] Sellier A (2003) Migration of an insulating particle under the action of uniform ambient electric and magnetic fields. part 2. boundary formulation and ellipsoidal particles. J Fluid Mech 488:335–353. https://doi.org/10.1017/S0022112003004944
[142] Takahashi K, Taniguchi S (2003) Electromagnetic separation of nonmetallic inclusion from liquid metal by imposition of high frequency magnetic field. ISIJ Int 43:820–827. https://doi.org/10.2355/isijinternational.43.820
[143] Damoah LNW, Zhang L (2016) High frequency electromagnetic separation of inclusions from aluminum. In: Suarez CE (ed) Light metals 2012. Springer, Cham, pp 1069–1076. https://doi.org/10.1007/978-3-319-48179-1_185
[144] Li K, Wang J, Shu D, Li TX, Sun BD, Zhou YH (2002) Theoretical and experimental investigation of aluminum melt cleaning using alternating electromagnetic field. Mater Lett 56:215–220. https://doi.org/10.1016/S0167-577X(02)00442-1
[145] Shu D, Li TX, Sun BD, Wang J, Zhou YH (1999) Study of electromagnetic separation of nometallic inclusions from aluminum melt. Metall Mater Trans A 30:2979–2988. https://doi.org/10.1007/s11661-999-0135-4
[146] Shu D, Sun B, Li K, Zhou Y (2003) Particle trajectories in aluminium melt flowing in a square channel under an alternating magnetic field generated by a solenoid. Scripta Mater 48:1385–1390. https://doi.org/10.1016/S1359-6462(02)00654-1
[147] Li K, Shu D, Wang J, Du Z, Sun B, Zhou Y (2004) Theoretical study on separation of nonmetallic inclusion particles from a hollow cylindrical melt in alternating electromagnetic field. ISIJ Int 44:647–652. https://doi.org/10.2355/isijinternational.44.647
[148] Sun Z, Guo M, Vleugels J, Van Der Biest O, Blanpain B (2009) Numerical calculations on inclusion removal from liquid metals under strong magnetic fields. Prog Electromagn Res 98:359–373. https://doi.org/10.2528/Pier09100501
[149] Shin S, Jeon JB, Jang HS et al (2023) Effects of electromagnetic stirring process on melt quality of A356 aluminum alloy. Miner Process Extr Metall Rev 17:2652–2662. https://doi.org/10.1007/s40962-023-01052-3
[150] Zhang BW, Ren ZM, Wu JX (2006) Continuous electromagnetic separation of inclusion from aluminum melt using alternating current. Trans Nonferrous Met Soc China 16:33–38. https://doi.org/10.1016/S1003-6326(06)60006-X
[151] El-Kaddah N, Patel AD, Natarajan TT (1995) The electromagnetic filtration of molten aluminum using an induced-current separator. JOM 47:46–49. https://doi.org/10.1007/BF03221176
[152] Yaniao F, Sassa K, Iwai K, Asai S (1997) Separation of inclusions in liquid metal using fixed alternating magnetic field. Tetsu-to-Hagane 83:30–35. https://doi.org/10.2355/tetsutohagane1955.83.1_30
[153] Li C, Dang T, Gökelma M, Zimmermann S, Mitterecker J, Friedrich B (2023) Assessment of separation and agglomeration tendency of non-metallic inclusions in an electromagnetically stirred aluminum melt. In: Broek S (ed) Light metals 2023. TMS 2023. The minerals, metals & materials series. Springer, Cham, pp 906–914. https://doi.org/10.1007/978-3-031-22532-1_120
[154] Miki Y, Kitaoka H, Sakuraya T, Fujii T (1992) Mechanism for separating inclusions from molten steel stirred with a rotating electro-magnetic field. ISIJ Int 32:142–149. https://doi.org/10.2355/isijinternational.32.142
[155] Tanaka Y, Sassa K, Iwai K, Asai S (1995) Separation of nonmetallic inclusions from molten metal using traveling magnetic field. Tetsu-to-Hagane 81:1120–1125. https://doi.org/10.2355/tetsutohagane1955.81.12_1120
[156] Zhong Y, Ren Z, Deng K, Jiang G, Xu K (1999) Effect of distribution of magnetic flux density on purifying liquid metal by travelling magnetic field. J Shanghai Univ (Engl Ed) 3:157–161. https://doi.org/10.1007/s11741-999-0050-3
[157] Asai S (2000) Recent development and prospect of electromagnetic processing of materials. Sci Technol Adv Mater 1:191–200. https://doi.org/10.1016/S1468-6996(00)00016-4
[158] Yoon EP, Choi JP, Kim JH, Nam TW, Kitaoka S (2002) Continuous elimination of Al_2O_3 particles in molten aluminium using electromagnetic force. Mater Sci Technol 18:1027–1035. https://doi.org/10.1179/026708302225005909
[159] Xu Z, Li T, Zhou Y (2007) Continuous removal of nonmetallic inclusions from aluminum melts by means of stationary electromagnetic field and DC current. Metall Mater Trans A 38:1104–1110. https://doi.org/10.1007/s11661-007-9149-y
[160] Alemany A, Argous JP, Barbet J, Ivanes M, Moreau R, Poinsot S (1983) Electromagnetic device for the separation of inclusions contained in an electrically conductive fluid. French Patents, No. 80400.
[161] Zhao Z, Chai Y, Zheng S, Wang L, Xiao Y (2017) Electromagnetic field assisted metallic materials processing: a review. Steel Res Int 88:1600273. https://doi.org/10.1002/srin.201600273
[162] Wu J, Djavanroodi F, Gode C, Attarilar S, Ebrahimi M (2022) Melt refining and purification processes in Al alloys: a comprehensive study. Mater Res Express 9:032001. https://doi.org/10.1088/2053-1591/ac5b03
[163] Kvithyld A, Syvertsen M, Bao S et al (2019) Aluminium filtration by bonded particle filters. In: Chesonis C (ed) Light metals 2019. The minerals, metals & materials series. Springer, Cham, pp 1081–1088. https://doi.org/10.1007/978-3-030-05864-7_132
[164] Bergin A, Voigt C, Fritzsch R et al (2022) Performance of regular and modified ceramic foam filters (CFFs) during aluminium melt filtration in a pilot-scale setup. In: Eskin D (ed) Light Metals 2022. Springer, Cham, pp 640–648. https://doi.org/10.1007/978-3-030-92529-1_84
[165] Olson IIIRA, Martins LCB (2005) Cellular ceramics in metal filtration. Adv Eng Mater 7:187–192. https://doi.org/10.1002/adem.200500021
[166] Damoah LNW, Zhang L (2010) Removal of inclusions from aluminum through filtration. Metall Mater Trans B 41:886–907. https://doi.org/10.1007/s11663-010-9367-3
[167] Gaustad G, Olivetti E, Kirchain R (2012) Improving aluminum recycling: a survey of sorting and impurity removal technologies. Resour Conserv Recycl 58:79–87. https://doi.org/10.1016/j.resconrec.2011.10.010
[168] Ali S, Apelian D, Mutharasan R (1985) Refining of aluminum and steel melts by the use of multi-cellular extruded ceramic filters. Can Metall Q 24:311–318. https://doi.org/10.1179/cmq.1985.24.4.311
[169] Engh T, Rasch B, Bathen E (2016) Deep bed filtration theory compared with experiments. In: Grandfield JF, Eskin DG (eds) Essential readings in light metals. Springer, Cham, pp 263–270. https://doi.org/10.1007/978-3-319-48228-6_32
[170] Voigt C, Fankhänel B, Jäckel E, Aneziris CG, Stelter M, Hubálková J (2015) Effect of the filter surface chemistry on the filtration of aluminum. Metall Mater Trans B 46:1066–1072. https://doi.org/10.1007/s11663-014-0232-7
[171] Voigt C, Dietrich B, Badowski M, Gorshunova M, Wolf G, Aneziris CG (2019) Impact of the filter roughness on the filtration efficiency for aluminum melt filtration. In: Chesonis C (ed) Light metals 2019. The minerals, metals & materials

series. Springer, Cham, pp 1063–1069. https://doi.org/10.1007/978-3-030-05864-7_130
[172] Voigt C, Fankhänel B, Dietrich B et al (2020) Influence of ceramic foam filters with Al_2O_3 nanocoating on the aluminum filtration behavior tested with and without grain refiner. Metall Mater Trans B 51:2371–2380. https://doi.org/10.1007/s11663-020-01900-1
[173] Yang J, Bao S, Akhtar S, Shen P, Li Y (2021) Influence of grain refiners on the wettability of Al_2O_3 substrate by aluminum melt. Metall Mater Trans B 52:382–392. https://doi.org/10.1007/s11663-020-01989-4
[174] Apelian D, Choi KK (1988) Metal refining by filtration. In: Katz S, Landefeld CF (eds) Foundry processes. Springer, Boston, MA, pp 467–493. https://doi.org/10.1007/978-1-4613-1013-6_19
[175] Gauckler LJ, Waeber MM, Conti C, Jacob-Duliere M (1985) Ceramic foam for molten metal filtration. JOM 37:47–50. https://doi.org/10.1007/BF03258640
[176] Laé E, Duval H, Rivière C, Le Brun P, Guillot JB (2016) Experimental and numerical study of ceramic foam filtration. In: Grandfield JF, Eskin DG (eds) Essential readings in light metals. Springer, Cham, pp 285–290. https://doi.org/10.1007/978-3-319-48228-6_34
[177] Gauckler LJ, Waeber MM, Conti C, Jacob-Dulière M (2016) Industrial application of open pore ceramic foam for molten metal filtration. In: Grandfield JF, Eskin DG (eds) Essential readings in light metals. Springer, Cham, pp 251–262. https://doi.org/10.1007/978-3-319-48228-6_31
[178] Luo XX, Zhang HT, Chen DD, Cui JZ, Nagaumi H (2015) Numerical analysis of effect of filtration on removal of inclusions in AA3104 aluminum alloy. In: Proceedings of the 2015 6th International Conference on Manufacturing Science and Engineering Atlantis Press, https://doi.org/10.2991/icmse-15.2015.337
[179] Dai Y, Voigt C, Storti E et al (2024) Open-cell ceramic foam filters for melt filtration: Processing, characterization, improvement and application. J Mater Sci Technol 32:3402–3422. https://doi.org/10.1016/j.jmrt.2024.08.167
[180] Schoß JP, Baumann B, Keßler A, Szucki M, Wolf G (2023) Filtration efficiency in the recycling process of particle-reinforced aluminum alloys using different filter materials. Miner Process Extr Metall Rev 17:1681–1696. https://doi.org/10.1007/s40962-022-00880-z
[181] Towsey N, Schneider W, Krug HP, Hardman A, Keegan NJ (2016) The influence of grain refiners on the efficiency of ceramic foam filters. In: Grandfield JF, Eskin DG (eds) Essential readings in light metals. Springer, Cham, pp 291–295. https://doi.org/10.1007/978-3-319-48228-6_35
[182] Yang J, Bao S, Akhtar S, Tundal U, Tjøtta S, Li Y (2021) The influences of grain refiner, inclusion level, and filter grade on the filtration performance of aluminum melt. Metall Mater Trans B 52:3946–3960. https://doi.org/10.1007/s11663-021-02310-7
[183] Yang J, Xu Y, Bao S et al (2022) Effect of inclusion and filtration on grain refinement efficiency of aluminum alloy. Metall Mater Trans A 53:1000–1012. https://doi.org/10.1007/s11661-021-06570-5
[184] Yang J, Bao S, Akthar S, Li Y (2019) Study of controllable inclusion addition methods in Al melt. In: Chesonis C (ed) Light metals 2019. The minerals, metals & materials series. Springer, Cham, pp 1041–1048. https://doi.org/10.1007/978-3-030-05864-7_127
[185] Duval H, Rivière C, Laé É, Le Brun P, Guillot JB (2009) Pilot-scale investigation of liquid aluminum filtration through ceramic foam filters: comparison between coulter counter measurements and metallographic analysis of spent filters. Metall Mater Trans B 40:233–246. https://doi.org/10.1007/s11663-008-9222-y
[186] Instone S, Badowski M, Schneider W (2005) XC filter-A filter technology for increased filtration performance. 2005: 267-275
[187] Instone S, Badowski M, Schneider W (2005) Development of molten metal filtration technology for aluminium. Light Metals 2005:933–938
[188] Courtenay JH, Reusch F, Instone S (2011) Recent results with new filter technologies based on the principle of multi stage filtration with grain refiner added in the intermediate stage. Mater Sci Forum 693:169–178. https://doi.org/10.4028/www.scientific.net/MSF.693.169
[189] Apelian D, Mutharasan R (1980) Filtration: a melt refining method. JOM 32:14–19. https://doi.org/10.1007/BF03354512
[190] Voigt C, Jäckel E, Taina F et al (2017) Filtration efficiency of functionalized ceramic foam filters for aluminum melt filtration. Metall Mater Trans B 48:497–505. https://doi.org/10.1007/s11663-016-0869-5
[191] Voigt C, Wetzig T, Hubálková J, Gehre P, Brachhold N, Aneziris CG (2024) Ceramic filter materials and filter structures with active and reactive functional pores for the aluminum melt filtration. In: Aneziris CG, Biermann H (eds) Multifunctional ceramic filter systems for metal melt filtration. Springer Series in Materials Science, vol 337. Springer, Cham. https://doi.org/10.1007/978-3-031-40930-1
[192] Voigt C, Ditscherlein L, Werzner E et al (2019) Influence of the wetting behavior on the aluminum melt filtration. In: Chesonis C (ed) Light metals 2019. Springer, Cham, pp 1071–1079. https://doi.org/10.1007/978-3-030-05864-7_131
[193] Voigt C, Hubálková J, Zienert T et al (2020) Aluminum melt filtration with carbon bonded alumina filters. Materials 13:3962. https://doi.org/10.3390/ma13183962
[194] Ni H, Yu Z, Mingyu H, Weibiao G, Sun B (2006) Purifying effects and mechanism of a new composite filter. Mater Sci Eng A 426:53–58. https://doi.org/10.1016/j.msea.2006.03.078
[195] Wu Y, Yan H, Wang J, Zheng J, Na X, Wang X (2024) Research on online monitoring technology and filtration process of inclusions in aluminum melt. Sensors 24:2757. https://doi.org/10.3390/s24092757
[196] Sun BD, Ding WJ, Shu D, Zhou YH (2004) Purification technology of molten aluminum. J Cent South Univ Technol 11:134–141. https://doi.org/10.1007/s11771-004-0028-z
[197] Gao J, Guo Z (2024) General Introduction. In: Super gravity metallurgy. Springer, Singapore. https://doi.org/10.1007/978-981-99-4649-5_1
[198] Song G, Song B, Yang Y, Yang Z, Xin W (2015) Separating behavior of nonmetallic inclusions in molten aluminum under super-gravity field. Metall Mater Trans B 46:2190–2197. https://doi.org/10.1007/s11663-015-0403-1
[199] Song G, Song B, Yang Z, Yang Y, Zhang J (2016) Removal of inclusions from molten aluminum by supergravity filtration. Metall Mater Trans B 47:3435–3445. https://doi.org/10.1007/s11663-016-0775-x
[200] Wang Z, Wei Q, Hu M, Guo Z (2024) CFD simulation and water model experiments with overflow-type supergravity reactor set up for continuously removing inclusions from aluminum melt. Miner Eng 209:108640. https://doi.org/10.1016/j.mineng.2024.108640
[201] Sun B, Lan X, Wang Z, Sun N, Guo Z (2024) Grade-preserving recycling of highly polluted Al-Mg-Si alloys scrap: continuous filtration under supergravity-induced. Sustain Mater Technol 40:e00918. https://doi.org/10.1016/j.susmat.2024.e00918
[202] Song G, Song B, Yang Y, Jia S, Song M (2016) Separation of non-metallic inclusions from aluminum melt by super gravity.

In: Jiang T et al (eds) 6th International symposium on high-temperature metallurgical processing. Springer, Cham, pp 715–722. https://doi.org/10.1007/978-3-319-48217-0_91